PDC DRILL BIT MODELING

IN HARD ROCK

By

SETH SLEEPER

Bachelor of Science in Mechanical Engineering

Oklahoma State University

Stillwater, Oklahoma

2018

Submitted to the Faculty of the
Graduate College of the
Oklahoma State University
in partial fulfillment of
the requirements for
the Degree of
MASTER OF SCIENCE
May, 2020

PDC DRILL BIT MODELING

IN HARD ROCK

Thesis Approved:

Dr. Geir Hareland

Thesis Adviser

Dr. Runar Nygaard

Dr. Prem Bikkina

ACKNOWLEDGEMENTS

I would like to first and foremost thank my advisor Dr. Geir Hareland for giving me the opportunity to be a part of the Oklahoma State University petroleum engineering master's program. The research I was able to take part in could not have been completed without his guidance and continual efforts to set me up for success.

I would also like to thank Sandia National Laboratories for providing their time and resources to ensure this research could be completed. In addition, I would like to show my gratitude for the graduate research team: Amin Atashnezhad, Saman Akhtarmanesh, Doug Bridges, and Kevin Klein for their valuable input whenever I needed help along the way.

I would also like to thank my committee members Dr. Runar Nygaard and Dr. Prem Bikkina for their help in ensuring I had the resources and guidance I needed during my time in the petroleum engineering master's program.

Name: Seth Sleeper

Date of Degree: May, 2020

Title of Study: PDC DRILL BIT MODELING IN HARD ROCK

Major Field: PETROLEUM ENGINEERING

Abstract: The objective of thesis is to develop a detailed PDC drill bit ROP model that can be implemented in a real time drilling optimization system for hard rock application. Within the drilling industry, often times operational costs are in terms of run time or daily rates which makes the need to maximize the efficiency of time spent in drilling a well key to coming in under budget. This study is a part of a two year department of energy project interested in increasing efficiency in hard rock drilling operations to increase the economic viability for renewable energy developed by geothermal wells. The approach taken to develop the new PDC drill bit ROP model began with PDC single cutter performance modeling in hard rock which initiated the step by step process of full hole integration. In conjunction to this study, full hole testing was conducted at Sandia Nation Laboratories in their hard rock drilling facility where PDC drill bit performance was analyzed in Sierra White Granite. The results of this study verified a new PDC drill bit ROP model based on single cutter performance. In addition, implementation of the model on the experimental data showed prediction capabilities were sufficient with less than 1% error. The results indicate that single cutter integration along with bit performance parameters included in the model proved to be viable in the development of the real time optimization system.

TABLE OF CONTENTS

Chapter Page

LIST OF TABLES

Table Page

LIST OF FIGURES

Figure Page

Figure Page

Figure Page

CHAPTER I

INTRODUCTION

After Polycrystalline Diamond Compact (PDC) bits made their debut in the 1970's, the use of them has progressively dominated bit runs in the drilling industry. The performance of PDC bits revolutionized drilling operations with their efficiency and reliability. In addition, PDC drill bits have allowed the development of new drilling operations all over the world for both on and off shore drilling. PDC drill bits account for nearly 70% of all bit runs in the drilling industry today (bellin et al, 2010; Menand and Gerbaud 2005). Traditionally roller cone bits accounted for the majority of all drill bits used within the drilling industry. Roller cone bits incorporate mechanical structures that are free to roll as the bit rotates. The rotation allows for repetitive impaling of the rock which would result in breaking down the formation through crushing. The mechanical structures or cones, shown in Figure 1.1, are either designed with tungsten carbide studs which would be referred to as a button or insert bit, or solid steel which were known as milled tooth bits. Milled tooth bits were designed to be implemented in softer formations whereas the button bits could incorporate their more durable tungsten carbide studs to break down hard rock formations.

Figure 1.1: Example of roller cone button bit (left) and mill tooth bit (right) (Sheikhnejad et al. 2014)

For harder or more abrasive formations where roller cone bits lacked effectiveness Natural Diamond Bits (NDB), as seen in Figure 1.2, would often be used instead. NDB incorporate diamond inserts set in the bits surface to create an abrasive cutting face. The abrasive cutting face of these bits use grinding to break down the formation which make them limited to very minimal depths of cut (DOC) rendering them ineffective in softer formations if encountered.

Figure 1.2: Example of natural diamond bit (Wöhrl,and de Wall 2002)

PDC bits, shown in Figure 1.3, use their cutting structures to impale into a formation and through the rotation of the bit shear the rock. The incorporation of shearing is important because rocks need significantly less force to fail under shearing than by crushing. Not only do PDC bits provide a more effective rate of penetration (ROP), they are fixed structures with no mechanically attached features like roller cone bits. The fixed blade PDC design immediately limited non-productive time (NPT) from issues experienced from roller cone bits like bearings going bad or fishing operations that often occurred when a cone detached down hole.

Figure 1.3: Example of PDC bit (Liou 2012)

The solid structure of the PDC bit was made up of either a steel or matrix body. During the manufacturing of a PDC bit, recessed inserts are established at predesigned locations such that PDC cutters can later be attached through a metallurgical process called brazing. The PDC cutter, shown in Figure 1.4, consists of a tungsten carbon stud with the polycrystalline synthetic diamond table that becomes fused to the stud through metallurgical process called sintering.

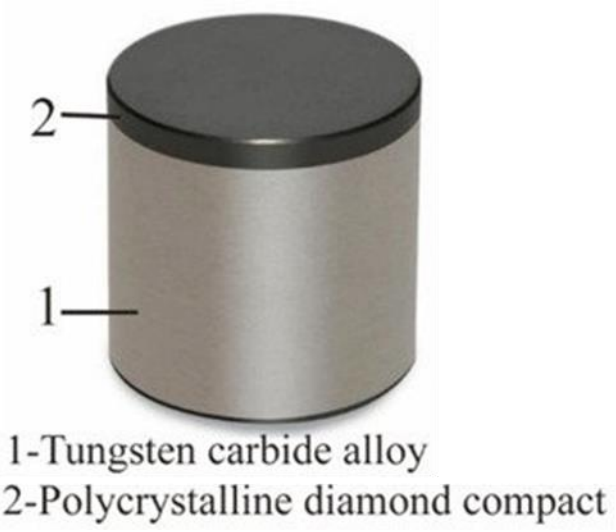

Figure 1.4: Example of PDC cutter (Lie et al. 2019)

Material improvements that increased PDC cutter performance include better diamond table development that decrease failures associated to impact or abrasiveness as well as higher temperature resistivity. The increase in temperature resistivity stems from a chemical process known as leaching which extracts unwanted materials such as cobalt that can increase the rate at which cutters begin to overheat. PDC cutter improvements have been instrumental in the effectiveness of PDC drill bit efficiency. Often times these improvements are analyzed and verified in lab testing since most drilling budgets cannot afford uncertainty in estimated bit performance. Much of these improvements are initially derived using rock cutter interaction modeling (Ernst and Merchant (1941); Glowka (1987); Detournay and Defourny (1992); Gerbaud et al. (2006); and Rahmani (2013)). The models listed use several different methods to help describe the rock cutter interface and the forces that need to be overcome for a single PDC cutter to be effective. To verify these models experimentally, single cutter testing must be conducted. These single cutter tests are typically conducted on what is known as a vertical turret lathe (VTL), as shown in Figure 1.5.

Figure 1.5: Single cutter VTL testing device with rock installed (Hellvik et al. 2012)

Testing conducted with a VTL has allowed for better understanding of cutter limitations and continual improvement of PDC cutter technology. As PDC cutter and bit technology improvements began to stack up, the traditional roller cone and NDB over time were unable to achieve similar reliability or performance compared to that of the PDC drill bits.

1.1 Drilling Today

PDC drill bits have affected the entire economy of the oil and gas industry in large part due to their longer bit life, increased ROP, and effectiveness in shale drilling applications. In the drilling industry, oftentimes, services and rentals are billed in terms of run time or daily rates.-With the performance gained by using PDC drill bits it becomes more evident of their financial impact to a successful drilling program. To capitalize on their financial impact, PDC drill bit performance is often simulated or modeled by a drilling team in the preplanning of a well's development. These ROP models help create a picture of the fastest and more efficient approach to completing a well under budget. A parameter often considered is the number of bits needed to reach a specific

location in the well, whether it is the kick off point (KOP) or the total depth (TD), so that tripping time can be estimated and worked into a budget. In the industry today, the fastest approach is almost always considered the most effective. In some scenarios, lowering weight on bit (WOB) and RPM would result in less wear and tear on the bit, as well as additional tools in the bottom hole assembly (BHA). The decrease in wear on the bit could potentially save a drilling program from having to make unforeseen additional trips for an additional bit rental or purchase to reach the remaining footage if operational parameters were too aggressive. With this in mind, ROP models now strive to incorporate real time ROP modeling to maximize efficiency and speed of each run to ensure a bit run reaches the estimated target.

1.2 Motivation

Traditional ROP modeling are vital when it comes to preplanning and post drilling analysis to optimize drilling operations. Many of these traditional ROP models (Bingham (1965); Hareland and Rampersad (1994); Motahhari et al. (2010); and Kerkar et al. (2014)) have been analytically/empirically developed in state of the art drilling labs to simulate drilling conditions under field application to increase accuracy. Due to hard rock behavior being more difficult to predict, the majority of the models developed direct their study at pure ductile failure as seen by softer rocks, such as shales, as it is more predictable. Using these ROP models that assume ductile failure on hard rock applications are inaccurate. As technology advances, more data are being captured and going unused within the industry. Advancements like wired drill pipe provide real time data that could be utilized in optimizing drilling operations through modeling. The developed model in this work is a key deliverable in the two-year project conducted to develop a real-time drilling optimization system for geothermal drilling application. A team of researchers from Oklahoma State University (OSU), University of Oklahoma, and Sandia National Laboratories (SNL) with funding from the Department of Energy (DOE) was assigned to conduct

the testing and model development necessary to create a real time drilling optimization system for hard rock. The finished project will deliver a model that includes drill stem vibrational analysis, Mechanical Specific Energy (MSE), and a detailed PDC drill bit model. These three components create a coupled system that estimates optimal WOB and RPM ranges to avoid drill stem vibrations while increasing the efficiency of the system utilizing ROP and/or MSE to ensure minimum required input in the system for maximum performance and equipment life. A visual representation of these coupled optimization parameters is shown in Figure 1.5.

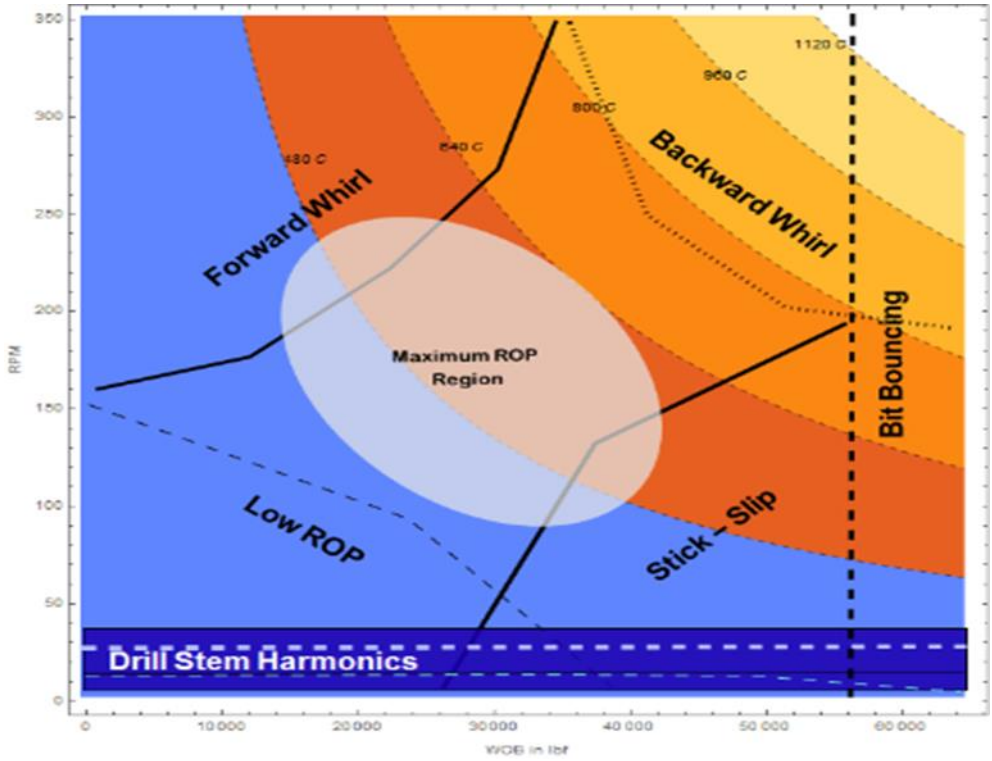

Figure 1.6: ROP Optimization System

The goal of this work is the development of the detailed PDC drill bit model that can be implemented in the real time drilling optimization system for hard rock drilling application.

CHAPTER II

REVIEW OF LITERATURE

2.1 Single Cutter Modeling

One of the earliest models to describe cutting of materials incorporating a cutter was developed by (Ernst and Merchant, 1941). The models primary purpose of development was targeted towards metal cutting. The reason the model has been adopted by many as a rock cutter model is that many formations under high confining pressure tend to behave in a ductile way such as a metal when sheared at lower DOC. This early model by Ernst and Merchant (1941) introduces a singular shear plane that assumes constant contact with the cutting surface and material. Their model includes a correlation for the tangential force (F_t) and axial force (F_a) as described below in Equation 2.1 and Equation 2.2.

$$F_t = \frac{\tau A \cos(\psi+\theta)}{\sin\alpha \cos(\alpha+\psi+\theta)} \tag{2.1}$$

$$F_a = F_t \tan(\psi + \theta) \tag{2.2}$$

Where:

F_t: Tangential force (lbf)

F_a: Axial force (lbf)

τ: Shear strength ($\mathrm{lb/ft^2}$)

A: Area of cut ($\mathrm{in^2}$)

θ: Cutter back rake angle (degree)

ψ: Interfacial friction angle between broken rock and cutter (degree)

α: Shear angle (degree)

By taking the partial derivative of the tangential force equation with respect to the shear angle, the following correlation in Equation 2.3 can be found that explains the relationship between cutter back rake angle, shear angle, and interfacial friction angle.

$$2\alpha + \psi + \theta = \frac{\pi}{2} \tag{2.3}$$

Using principles from the Ernst and Merchant (1941) model, Glowka's single cutter model expanded on the previous cutting models and correlated it to rock cutting. Glowka's (1987) model took many other factors into account such as estimation of cutting forces, temperature profiles, and the wear rate for PDC cutters. All of these factors were taken into consideration to provide a method that could be used to create a measurement described as a rock's "drillability". In addition, the force estimation model expands on sharp (no chamfer) and blunt single cutter analysis. Glowka (1987) experimentation showed how wet jetting assistance decreases the wear rate for the cutters as cutters are cooled more efficiently. The work was designed around geothermal drilling of hard rock that could also be translated into the petroleum industry. The experimentation began with the single cutter testing to understand the limitations of the PDC cutters. Once the limitations were understood then a design could be implemented for PDC cutters such that the cutters operate efficiently and wear evenly in harsh environments. The

factors that were taken into consideration for developing this model included properties such as: rock type, cutter design, and wear state. The lithologies of interest were Sierra White Granite, Tennessee Marble, and Berea Sandstone to cover a wide range of rock strengths. The drag forces were determined to be strongly dependent on the rock type, but relatively independent of depth of cut and wearflat area.

For blunt cutters,

$$\frac{F}{A_w} = C_1 \delta^{n1} \tag{2.4}$$

A_w: Wear area (in^2)

C_1,n1: Rock property constants

For sharp cutters,

$$F = C_2 \delta^{n2} \tag{2.5}$$

$$\mu_d = \frac{F_d}{F} \tag{2.6a}$$

$$F_d = \mu_d F \tag{2.6b}$$

Where:

F_d: Drag force (lbf)

F: Sharp cutter penetrating force (lbf)

μ_d: Cutter drag coefficient (-)

δ: Cutter depth of cut (in)

C_2, n2: Rock property constants

Using the data from the Glowka (1987) report shown in Table A-1 and Detournay and Defourny (1992) developed a model to describe the failure mode of sedimentary rocks at different depths of cut ranging from 0.001 to 0.01 inches. This model was developed under single cutter analysis looking at sharp cutters (no chamfer) and blunt cutters. The experimental data for Berea Sandstone and Sierra White Granite, used in their work, was the testing reported by Glowka (1987) under atmospheric conditions with unsaturated rock samples. This force model, branching from Glowka's studies, also uses the singular shear plane principal noted in the Ernst and Merchant (1941) model to define their sharp cutter force model. Some of the key assumptions to this model are; Torque (T) and WOB (W) are linearly proportional to specific energy (E) and drilling strength (S) which are dimensions of stress. The intrinsic specific energy (ε) is defined as roughly the unconfined compressive strength (UCS) of the rock which is used to describe the minimum amount of energy required to fail a unit volume of rock. Intrinsic specific energy has been found to be dependent of factors such as bottom-hole pressure, pore pressure, rock-cutter interfacial friction angle, and back rake angle of the cutter (Detournay et al., 2008).

Sharp cutter,

$$F_s^c = \varepsilon * A_c \tag{2.7}$$

$$F_n^c = \zeta * \varepsilon * A_c \tag{2.8}$$

$$\zeta = \tan(\theta + \psi) \tag{2.9}$$

Perfectly sharp cutters we have: $\varepsilon = E$ and $S = \zeta * \varepsilon$ (2.10) and (2.11)

Where:

A_c: Area of the cutter in contact with the rock (in^2)

F_n^c: Normal force (lbf)

F_s^c: Drag force (lbf)

ζ: Ratio of the normal and drag force (-)

ψ: Interfacial friction angle (degree)

ε: Intrinsic specific energy ($\mathrm{lb/in^2}$)

S: Drilling strength (lb/in^2)

Gerbaud et al. (2006) later developed a model incorporating a crushed zone of rock that fails the preceding formation as well as a chamfered cutter design into the force modeling. The chamfers on the cutting edge of a PDC cutter is used as an initial wearflat area that reduces the possibility of prematurely chipping the diamond table on the cutter. The buildup edge of crushed materials on the cutting face is assumed to be unique to the model as it shows how energy is transferred from the cutter, through the crushed material that is in contact with the rock. By using this assumption, it is not the cutter in direct contact with the rock that is causing the rock to fail as previously modeled, but that of the crushed material contact is responsible for the failure of the rock. The direct consequence of stating that that build-up edge induces the rock failure allows the model to use a constant single chip failure plane independent of PDC orientation. Since the rock failure characteristics for this model was assumed to be solely done by ductile failure and brittle failure is negligible, rock formations chosen were Vosges Sandstone and Buxy Limestone.

Sharp cutters,

$$F_c^c = \sigma_o * \left(1 + k * \tan(\varphi') * \tan(\omega_c)\right) * A \tag{2.12}$$

$$F_n^c = \sigma_o * \left(\tan(\theta_f) + k * \tan(\omega_c)\right) * A \tag{2.13}$$

$$\sigma_o = \frac{C_o + P_b * (\sin(\psi) * \cos(\psi) + cos^2(\psi) * \tan(\varphi)}{(1 - \tan(\theta_f) * \tan(\varphi)) * (\sin(\psi) * \cos(\psi) - \tan(\theta_f + \varphi) * sin^2(\psi))} \tag{2.14}$$

$$\tan(\varphi') = \frac{\pi}{2} * \tan(\varphi) \quad (2.15)$$

Where:

F_c^c: Tangential forces acting on the cutter (lbf)

F_n^c: Normal force acting on the cutter (lbf)

k: Ratio of horizontal contact surface of the crushed zone (-)

φ': Friction angle between the crushed rock and the virgin rock (degree)

ω_c: Back rake angle (degree)

A: Area in front of the cutter (in^2)

θ_f: Friction angle at the interface of the rock and cutter (degree)

σ_o: Hydrostatic stress in the crush material (lb/in^2)

P_b: Mud pressure (lb/in^2)

ψ: Single chip failure plane independent of PDC orientation (degree)

φ: Rock internal friction angle (degree)

Chamfer forces,

$$F_c^{ch} = \sigma_o * \tan(\varphi') * A_{ch} \quad (2.16)$$

$$F_n^{ch} = \sigma_o * A_{ch} \quad (2.17)$$

Where:

F_c^{ch}: Tangential forces acting on the chamfer (lbf)

F_n^{ch}: Normal force acting on the chamfer (lbf)

A_{ch}: Area in front of the chamfer (in^2)

Later, Rahmani in 2013 developed a new model is based off of the Ernst and Merchant (1941) cutting model but coupled parameters to allow the model to be used for rock cutting. An assumption that fine grained, impermeable rocks such as shales under high confining pressure behave much like metal when being sheared. This ductile shearing under confining pressure produces ribbon like cuttings. The Rahmani (2013) model quantifies the energy spent to overcome frictional forces on the shear plane, or the ribbon like cuttings. This was accounted for by adding an additional friction term to the model developed by (Ernst and Merchant, 1941).

Sharp cutters,

$$F_{CF} = \mu_c F_{Conf} \tag{2.18}$$

$$F_{Conf} = P_c A_s = P_c \frac{wd}{\sin(\alpha)} \tag{2.19}$$

$$F_t = \frac{wd}{\sin(\alpha)} (\tau_c + \mu_c P_c)(\frac{Cos(\psi+\theta)}{Cos(\alpha+\psi+\theta)}) \tag{2.20}$$

$$F_a = \frac{wd}{\sin(\alpha)} (\tau_c + \mu_c P_c)(\frac{sin(\psi+\theta)}{Cos(\alpha+\psi+\theta)}) \tag{2.21}$$

$$\tau_c = CP_c tan(\varphi) \tag{2.22}$$

Where:

F_{CF}: Force on the cuttings due to friction (lbf)

μ_c: Friction coefficient between the cuttings and intact rock along the shear plane (-)

F_{Conf}: Normal forces acting on the cuttings upper surface (lbf)

P_c: Bottom hole confining pressure ($\mathrm{lb/in^2}$)

A_s: Shear plane ($\mathrm{in^2}$)

w: Width of the cut (in)

d: Depth of cut (in)

α: Shear stress angle (degree)

ψ: Interfacial friction angle between the broken rock and cutter (degree)

τ_c: Confined shear strength of the rock ($\mathrm{lb/in^2}$)

C: Cohesiveness of the rock ($\mathrm{lb/in^2}$)

φ: Internal friction angle of the rock (degree)

2.1.1 Effects of Back and Side Rake Angles

As shale plays began to become more economically viable, issues associate to formations like fine grained shales began to limit performance of the PDC bits. The main issue associated to this limitation was known as “bit balling”. Huang and Iverson (1981) conducted a study to show the impact side rake has on effectively increasing efficiency of bit cleaning in soft or plastic formations to limit the bit balling. As descried by Huang and Iverson (1981), if cleaning is not done efficiently enough the shale cuttings will pack up the low velocity areas and from this point cleaning the tightly packed chip conglomeration is near impossible. Since shale makes up the majority of formations drilled, bit balling issues kept PDC bits in limited commission until more efficient cleaning methods could be developed to make them suitable tools for drilling shale formations. A visual representation of balled bits are shown in Figure 2.1 and Figure 2.2.

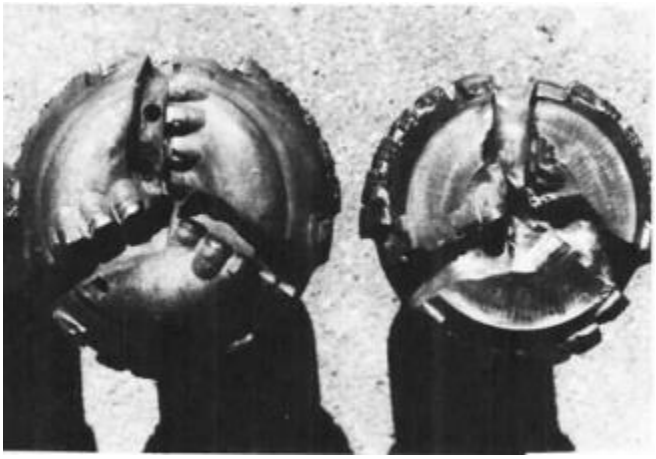

Figure 2.1: Premature wear of bits due to large fluid area (Huang and Iverson 1981)

Figure 2.2: Buildup of tightly packed shale particles on the blades of a balled bit (Huang and Iverson 1981)

Implementing a side rake to a metal cutting tool aids in the removal of metal cutting buildup in front of the cutting contact point. As previously stated by Rhamadi (2013) shale formations under high confining pressures are often modeled similarly to that of metal cutting, adding side rake on cutters in shales should follow the same principals for cutting removal. This means implementing

a side rake to a PDC cutter should enhance cutting evacuation which would limit the cutting buildup that creates the low velocity hydraulic zones. The results found in the Huang and Iverson (1981) study indicate a larger weight on bit to overcome side rake effects that limit the ability to maintain depth of cut are negligible. The main benefit described in Huang and Iverson (1981) is the mechanical cleaning action that comes from inducing a side rake while cutting. The tangentially and radially produced forces evacuate generated cuttings more effectively. It was also noticed that the larger the side rake the less likely it was that the chips tended to stick to the face of the cutter.

Rajabov et al. (2012) developed correlations to MSE when back rake and side rake are adjusted. MSE is a parameter that is used to quantify the minimum amount of energy needed to maintain penetration rate efficiency while not being too aggressive with input parameters. These tests were run under atmospheric conditions along with tests ran under confining pressures. The test results depict MSE decreases as the DOC increases up to 0.08 inches for both atmospheric and confining pressure tests for Carthage Marble, Mancos Shale, and Torrey Bluff Sandstone. One main point in the study indicated after the listed DOC of 0.08 inches is reached the MSE starts increasing again alluding to a possible optimum DOC. The study also showed that although Mancos Shale and Carthage Marble have roughly the same UCS, the Mancos Shale require three times less energy to fail the rock than what the Carthage Marble did. This also shows how compressive strengths for shales versus hard rocks differ when it comes to ductile and brittle failure modes along with the rocks' cohesiveness. One study found that increasing the back rake angle also increases the MSE. This would make sense due to the additional amount of normal force needed to reach the same DOC for larger back rake angles. When it comes to the back rake versus the MSE under atmospheric and confining pressure testing, the MSE still increased with the same magnitude as the back rake increased. The reported results from Rajaboy et al. (2012) of MSE versus back rake under confining pressure is shown in Figure 2.3.

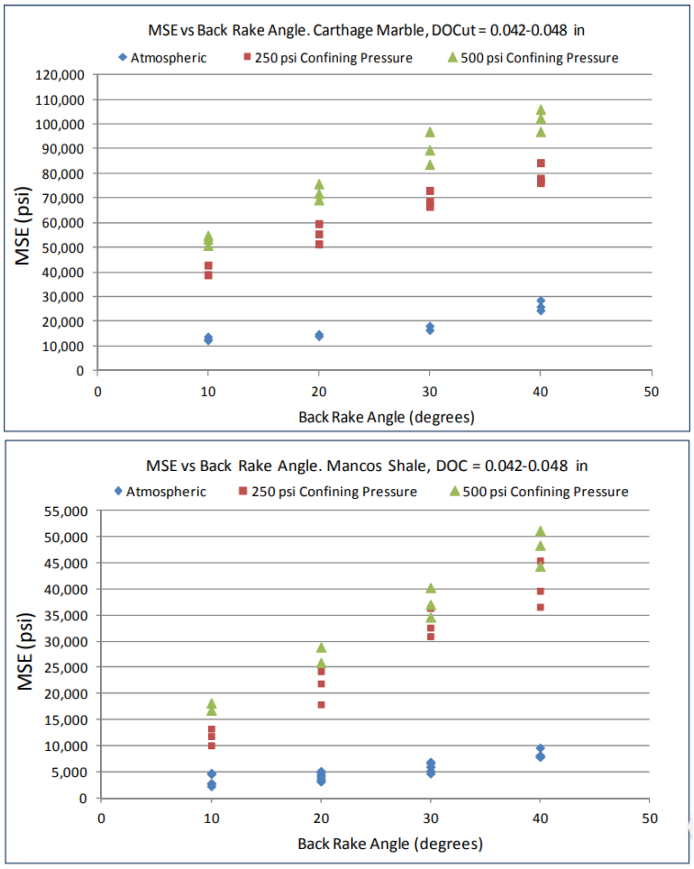

Figure 2.3: Effects of back rake angle on MSE for PDC cutters in Carthage marble (top) and Mancos shale (bottom) (Rajabov et al. 2012)

As for MSE versus side rake, the reported results in Figure 2.4 indicated side rake was negligible from 0 to 30 degrees compared to when the angles were from 30 to 60 degrees. The tests were run with a chamfered cutter with a depth of cut around 0.045 inches.

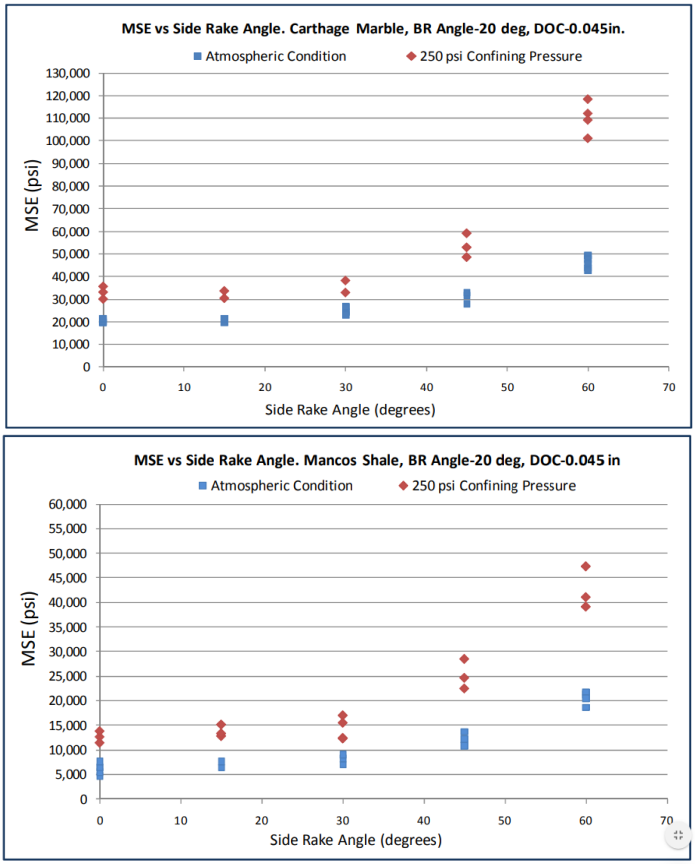

Figure 2.4: Effects of side rake angle on MSE for PDC cutters in Carthage marble (top) and Mancos shale (bottom) (Rajabov et al. 2012)

To develop an accurate physical ROP model an accurate representation of rock/cutter interaction needs to be established as well. There are limited number of models that can accurately depict what is happening for all the cutters in contact with the rock at once, but some of the fundamental properties that are covered in the previous models give a better indication of how ROP models are developed and tested for accuracy.

2.2 Rate of Penetration Modeling

The Bingham model developed in 1965 was one of the first ROP models developed to mathematically quantify ROP for drilling applications. Empirically calibrated coefficients (a) and (b) are variables that allow for rock properties for different lithologies to be taken into account.

$$ROP = aRPM\left(\frac{WOB}{D_B}\right)^b \tag{2.23}$$

Where:

RPM: Rotary speed of bit (Revolution/min)

D_B: Bit diameter (in)

WOB: Weight on bit (klbf)

$a,\ b$: Lithology constants

Though this model laid the ground work for ROP models to come, for today's standards it lacks key parameters due to progression in the design of PDC technology and a better understanding of materials that are key to more accurately predict PDC bit limitations. Some of these variables that should be included are bit type, bit wear, cutter design, cutter density, cutter orientation, hydraulics, and other variables associated with physical properties of the formation.

In 1994 Hareland and Rampersad developed a predictive drag bit ROP model that proved useful for the preplanning of wells, post drilling analysis, and drilling optimization. Given the data requirements, this model was designed to predict penetration rates for any set of operating conditions, formation descriptions, and bit parameters. Some of the parameters of interest for this model would include: bit mechanical design parameters, cutter geometrical descriptions, formation properties, cutter wear and operating conditions. The usefulness of the model is unique

as the parameters needed can be found in readily available data given lithology coefficients are known from either lab data, drill-off testing or bit performance tests that can be conducted in the field. The model utilizes single cutter rock interaction to create the foundation of the model which is then extrapolated into a full hole design. For different drag bit cutters A_v is subject to change.

$$ROP = W_f * COR * \frac{14.14 * N_s * RPM * A_v}{D_B} \tag{2.24}$$

RPM: Rotary speed of bit (Revolution/min)

N_s: Number of cutters (-)

A_v: Area of rock compressed ahead of a cutter (in^2)

D_B: Diameter of the bit (in)

$$A_v = cos(\alpha) sin(\theta) \left[\left(\frac{d_c}{2}\right)^2 cos^{-1}\left(1 - \frac{2P}{cos(\theta)\pi * d_c}\right) - \sqrt{\left(\frac{d_c P}{cos(\theta)} - \frac{P^2}{cos^2(\theta)}\right)\left(\frac{d_c P}{2cos(\theta)}\right)} \right] \tag{2.25}$$

$$P = \frac{2WOB}{\pi d_c \sigma_c} \tag{2.26}$$

d_c: Diameter of the cutter (in)

θ: Back rake angle (degree)

α: Side rake angle (degree)

P: Cutter penetration (in)

σ_c: Uniaxial compressive strength (lb/in^2)

Furthermore, from their model they described several phenomena that cannot be accurately accounted for theoretically in their modeling. Some of these effects would include rock strain rate, hydraulic efficiency for bit cleaning, and imperfections in overall bit and/or cutter geometry. Due to these factors not being accounted for, a simple, yet accurate and usable correction factor

(COR) was introduced. An overall lithology empirical correction factor (a), a bit rotational correction factor (b), and a mechanical weight on bit empirical correction factor (c) were incorporated in the equation listed below.

$$COR = \frac{a}{(RPM^b * WOB^c)} \tag{2.27}$$

WOB: Weight on bit (klbf)

RPM: Rotary speed of bit (Revolution/min)

a, b, c: Empirical coefficients

Based on the Hareland and Rapmersad (1994) model, a comprehensive ROP model was developed by Motahhari et al. (2010) which was designed to improve the drilling efficiency with positive displacement motors (PDM) in conjunction with PDC bits. The bit coefficient (G) was developed to determine various aspects of bit parameters such as: bit geometry, cutter size, cutter design including back rake and side rake angles, and a rock/cutter coefficient of friction. These expressions are as listed below.

$$ROP = W_f * (\frac{G * RPM_t^{\gamma} * WOB^{\alpha}}{D_B * S}) \tag{2.28}$$

Where:

RPM_t: Total bit rotary speed (Revolution/min)

D_B: Bit diameter (in)

S: Confined rock strength (lb/in^2)

γ, α: Empirical coefficients

The model assumes perfect bit cleaning efficiency which allows for a more predictable wear function as shown Equation 2.29. ROP constantly decreases due to the PDC cutters wearing down over the course of a bit run. Because of this, a dimensionless wear function (W_f), using experimental data reported by Glowka (1987), was developed to estimate the ROP reduction due bit wear so an entire bit run could be estimated. Numerical constants(K_{wf}), (ρ), (τ) were reported by (Motahhari et al., 2010).

$$W_f = K_{wf} * \left(\frac{WOB}{N_c}\right)^{\rho} * \frac{1}{S^{\tau} * {A_w}^{\rho+1}} \tag{2.29}$$

Where:

A_w: Wearflat area underneath of a single cutter (in^2)

N_c: Number of PDC cutters on the bit face (-)

K_{wf}, ρ, τ: Cutter empirical coefficients

A correlation made to rock strength was developed to estimate the strength of the rock under wellbore conditions. Empirical constants (a_s) and (b_s) are used to explain different lithologies as reported by (Rampersad, 1994).

$$S = S_0 * \left(1 - a_s {P_c}^{b_s}\right) \tag{2.30}$$

S_0: Unconfined compressive strength

P_c: Confining pressure

a_s, b_s: Rock strength empirical coefficients

A short time later a PDC bit ROP model was developed by Kerkar et al. (2014) that incorporates hydraulic performance, blade performance, and a wear function which made a comprehensive

model unlike most. The experimental data used to calibrate the model were reported by Warren and Armagost (1988) drill bit prototype experimentation performed on a variety of formations which include: Indiana limestone, Carthage limestone, Berea sandstone, Mancos shale, and Catoosa shale. Important terms within the PDC bit ROP model to describe various bit efficiency parameters include: an empirical wear function (W_f), wellbore cleaning efficiency based on bit hydraulics ($h(x)$), and a function used to calculate drilling inefficiencies due to blade count ($b(x)$).

$$ROP = \left[\frac{K1 * WOB^{a1} * RPM^{b1} * cos(SR)}{CCS^{c1} * D_B * tan(BR)}\right] * W_f * h(x) * b(x) \quad (2.31)$$

Where:

WOB: Weight on bit (klbf)

RPM: Rotary speed of bit (Revolution/min)

CCS: Confined compressive strength of the rock ($\mathrm{lb/in^2}$)

BR: Back rake (degree)

SR: Side rake (degree)

$K1$, $a1$, $b1$, $c1$: Drilling performance in varying lithology empirical coefficients

The empirical wear function (W_f) shown by Equation 2.33 was derived utilizing a bit dull grade correlation (ΔBG). The dull grade correlation is shown below in Equation 2.32.

Where (ΔBG) is the bit dull grade that ranges from 0 for a new bit to 8 for a completely worn bit.

$$\Delta BG = \mathrm{Ca} \sum_{i=2}^{n} WOB_i * RPM_i * CCS_i * ABR_i \quad (2.32)$$

ABR: Formation abrasiveness (-)

Ca: Cutter empirical coefficient

Once the dull grade parameters are accounted for, the correlation is then applied to the calibrated wear function shown below.

$$W_f = 1 - a_3 \left[\frac{\Delta BG}{8}\right]^{b_3} \tag{2.33}$$

a_3, b_3: Cutter empirical coefficients

The cleaning efficiency model $h(x)$ incorporates hydraulic empirical coefficients (a_2), (b_2), and (c_2) which were determined based off of laboratory testing under simulated borehole conditions reported in (Warren and Armagost (1988) and Holster and Kipp, (1984)).

$$h(x) = a_2 * \frac{(HSI * \frac{JSA}{2 * D_B})^{b_2}}{ROP^{c_2}} \tag{2.34}$$

HSI: Hydraulic performance of the bit ($\mathrm{hp/in^2}$)

JSA: Junk slot area ($\mathrm{in^2}$)

D_B: Bit diameter (in)

ROP: Rate of penetration based off perfect cleaning conditions ($\mathrm{ft/hr}$)

a_2, b_2, c_2: Hydraulic empirical coefficients

HSI as shown in Equation 2.35 is estimated by hydraulic horsepower (HHP) generated through a mud motor and dividing it by the area of the face of the bit (A_B). Additionally, this is a function that takes into account the flow rate (Q) and the pressure drop across the bit (P_B) generated by bit nozzles which can vary in size.

$$HSI = \frac{HHP}{A_B} = \frac{\frac{Q * P_B}{1714}}{\left(\frac{\pi}{4}\right) {D_B}^2} \tag{2.35}$$

HHP: Hydraulic horsepower (hp)

A_B; Area of the face of the bit (in^2)

Q: Flow rate (Gallon/min)

P_B: Pressure drop across the bit (lb/in^2)

D_B: Bit diameter (in)

It is said in the study that an increase in the number of blades leads to a decrease in drilling efficiency. To account for this Equation 2.36 was empirically developed to estimate the inefficiencies associated to the number of blades.

$$b(x) = \frac{RPM^{1.02-0.02N_b}}{RPM^{0.92}} \tag{2.36}$$

N_b: Number of blades (-)

RPM: Rotary speed of bit ($\text{Revolution}/\text{min}$)

The governing equation associated to rock strength shown by Equation 2.37 was empirically calibrated to estimate rock strength due to confining pressures in the wellbore.

$$UCS = \frac{CCS}{1+a_s * {P_c}^{b_s}} \tag{2.37}$$

P_c: Confining pressure (lb/in^2)

a_s, b_s: Fluid density empirical coefficients

2.2.1 Equivalent Radius

To eliminate modeling every cutter over the face of a PDC bit, a term known as equivalent radius was developed by Hareland and Rampersad (1994) for drag bit ROP models. They used this term to establish a mass balance over the face of a drag bit design. The area of the face of the bit is broken down into two zones as shown in Figure 2.5 where, the assumption is made that the amount of work required to remove the same volume of rock for both (A_1) and (A_2) equal for full bits (Hareland and Rampersad, 1994).

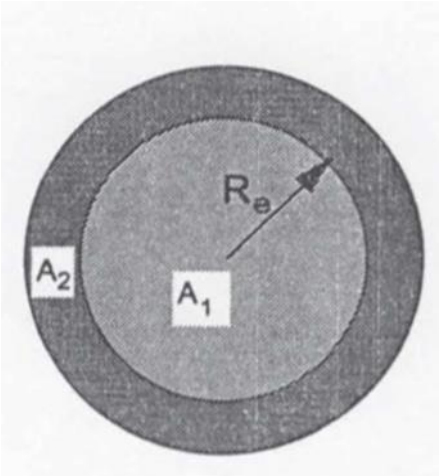

Figure 2.5: Equivalent radius concept (Hareland and Rampersad 1994)

Where equivalent radius (Re) is expressed in Equation 2.38.

$$Re = \frac{D_B}{2*\sqrt{2}} \quad (2.38)$$

Re: Equivalent radius (in)

D_B: Bit diameter (in)

2.2.2 PDC Bit Optimization

The developed drag bit performance modeling by Warren and Sinor (1989) was a guideline to help aid in bit selection. The evaluation process tries providing a baseline that helps identify and quantify variables that influence bit performance, but mainly cutter density. In their papers multiple tests have been evaluated by (Warren and Armagost 1988, Huang and Iverson 1981, Warren Sinor 1986) where much of their work was evaluating tests conducted on four different bits of all different geometry and cutter sizes. The model that was incorporated in their study was then applied to their previous experimental data. The model predictions were considered to be fairly good as long as hydraulic cleaning efficiency was maintained. Once the predictive model was verified, they conducted a test on if their model would still be accurate by adjusting only the number of cutters. This adjustment in cutter density was a product of removing four cutters at a time to see if this simple study adjusted the ROP by eliminating cutter interaction. Once cutters were removed to eliminate cutter interaction, each cutter that remained experienced higher loading which increased the volume of cuttings generated by each cutter. Their model estimated as cutters were removed a predicted increase in ROP which matched well with the cutter removal experimental results which showed a steep increase of ROP.

Later Sinor et al. (1998) used the effects of cutter density, back rake angle, cutter diameter, and the speed of the steady state wear rate on PDC cutters to study multiple aspects of rock failure. The aim was to understand these parameters and use them in the designing of PDC bits. The results listed by Sinor et al. (1998) indicate that for hard rocks, the penetrating stresses on the order of the compressive rock strength must be imposed on the rock surface before significant penetration occurs. For much softer formations like Berea Sandstone, it was indicated that significant penetration can be achieved with penetrating stresses much lower than the compressive rock strength. These findings are consistent with a similar study reported by Glowka

(1989). This means softer rocks do not require the same initial crushing of the rock surface that is required by hard rocks to achieve an optimal DOC.

The Mensa-Wilmot et al. (2003) study took up evaluating the limitations associated to PDC bits in hard and abrasive formations where they still lack effectiveness in some cases. The study analyzed parameters that would improve PDC bit life and ROP. According to the Mensa-Wilmot et al. (2003) paper, traditionally the industry standard of the best way to drill a hard and abrasive formation was to increase blade count and diamond volume. To increase the diamond volume, the diameter of the cutters would need to decrease to allow for more cutters on each blade to be implemented. It was speculated that in hard and abrasive formations two things are needed; maximized axial and radial diamond volume distributions. Additionally, quantifying term "hard" for hard rock formations was evaluated to set a baseline of what the term meant. The term hard was adopted when PDC technology was in the early stages of combating inefficient drilling in formations where many advancements had been made since. The term this paper adopted, from the Glowka (1987) study, and promotes is "drillability" which refers to the drilling difficulty and is not related to hardness. In support of this idea formations of the same hardness may not have the same lithology, this gives both compared formations different drilling challenges. The development portion of this paper is all theoretical and explains the limitations to the bits on the market and what the paper refers to as NPDC (New Polycrystalline Diamond Compact) bits. From then a strictly theoretical bit and cutter design practices are established such that a baseline could be established if development of a NPDC bit be taken up. Parameters of interest include: cutter orientation, number of cutter rows per blade, varying back rakes, and varying cutter sizes on each blade.

The study conducted by Hareland et al. (2009) analyzed improvements needed for efficiently drilling hard formations for geothermal applications. Geothermal energy requires deep drilling with considerable depths of up to +3km. If the efficiency of drilling through these hard formation

is increased, then the cost of drilling such a well decreases. As stated in Hareland et al. (2009) cutting efficiency of a single PDC is defined as the ratio of the volume removed by the cutter over the force required to remove that volume of rock shown by Equation 2.39. This relationship is a function of the back rake angle, depth of cut, and rock properties. With these parameters in mind, calculation of chip generation and the force required to generate said chip could be quantified.

$$Specific\ Volume = \frac{Volume\ of\ rock\ removed\ in\ one\ major\ chip}{Maximum\ force\ required\ to\ remove\ that\ volume\ of\ rock} \quad (2.39)$$

The relationship is then derived using complex geometry and compared to back rake angle and DOC. In conclusion, specific volume was most efficient when the back rake angle ranged from 0 to 25 degrees in the hard rock lithology analyzed. Specific volume compared to DOC indicated the larger DOC, the higher the cutting efficiency with the limiting factor being the exposure of the cutters themselves. For the experimentation that was conducted in this study the optimum DOC for the PDC bit used ranged from 0.04 to 0.06 inches.

2.3 Hydraulic Efficiency

During the drilling operation, deviations in a linear response between WOB and ROP can be interrupted by a multitude of different variables. One being the relationship of the drilling fluid and its ability to efficiently remove cuttings from around the drill bit. The point at which the hydraulics begin to limit the ROP response is known as the flounder point. Once this point is reached, understanding how to overcome the flounder point and create higher ROP becomes pertinent for drilling optimization.

Lab experimentation conducted by Holster and Kipp (1984) analyzed hydraulic horsepower's influence on drilling performance. In their experimentation, a range of drilling conditions were used and implemented on various rock types. Findings associated to their studies indicated that the hydraulic horsepower played a key role in drilling performance. Additionally, the main

finding was its not how much horsepower per square inch (HSI) could generated through the bit nozzles, but the rock/fluid combination where oil-based and water-based drilling fluids were key parameters. According to Holster and Kipp (1984), until their study very little had been published concerning the specific level of bit hydraulic energy or horsepower that is needed to maximize drilling rates. For the testing, the bit used was an 8.5-inch steel bodied PDC bit with five interchangeable nozzles including four sets of nozzles ranging from 8/32 to 11/32 inch. The rocks chosen include Mancos Shale, Pierre Shale, and Berea Sandstone so that a comprehensive analysis of mud and rock interactions could be determined. The drilling fluids were both 10-lbm/gal mixtures were kept relatively similar in terms of density, plastic viscosity, yield point, and filtration where the water-based fluid was a bentonite/lignosulfonate and the oil-based relaxed filtrate. Equation 2.40 was used to calculate hydraulic horsepower.

$$P_H = \frac{Q\Delta p}{1{,}714} \tag{2.40}$$

Q: Flow rate (gallon/min)

Δp: Pressure drop across the bit face ($\mathrm{lb/in^2}$)

The bit (HSI) or horsepower per square inch is a term often used to quantify hydraulic output through the nozzles of the bit. This estimation can be found using Equation 2.41.

$$HSI = \frac{4P_H}{\pi d^2} \tag{2.41}$$

P_H: Hydraulic horsepower (hp)

d: Bit diameter (in)

The results showed that HSI played a significant impact on the penetration rates in all of the testing, but the main impact was seen with the formation response the drilling fluids. Mancos Shale results showed both fluid types had similar response in penetration rates, but experienced bit balling under water-base mud whereas no bit balling occurred for the oil-based muds even at lower HSI values. Pierre Shale, a much softer gumbo like formation had a significant issue with bit balling when it came to the water-based muds reacting with the clay content of the rock. Oil-based mud was a must when it came to Pierre Shale due to the mud inhibiting the shale cuttings from sticking to themselves or the bit itself. Berea Sandstone, much like the Mancos Shale, saw little response in differing mud types as the formation is a chemically inert rock.

Testing conducted in 1987 by Warren also looked into hydraulic effects on penetration rates. Oil-based and water-based muds were also analyzed where interesting findings showed that oil-based muds in both Indiana and Carthage Limestone created a drilling response that made the rocks appear stronger than that they were in water-based testing. This response correlated in these formations being drilled considerably slower than the water-based counterpart. Tests ran in Mancos Shale showed similar results to Holster and Kipp (1984) where the two different fluids only slightly effected the penetration rates. Though it was mentioned at lower WOB ranges water-based muds appeared to drill faster whereas at the highest end of the WOB range oil-based mud performed better. It could be concluded from field testing in conjunction to their work that oil-based mud was the obvious option as the oil-based mud showed a reduction in hydrostatic head reducing overburden stresses on the formation. Additionally, in the field application higher WOB ranges were used where the lab testing implied better penetration rates at higher WOB similar to field application.

CHAPTER III

EXPERIMENTAL METHODOLOGY AND TESTING

This chapter describes the modeling and the data sets obtained from previously completed experimental work for single cutter and full hole analysis. To begin, single cutter modeling and the general test set up for the obtained data sets will be addressed. The single cutter force model implemented for this study and findings associated to the model will then be provided. Following this the full hole testing facility utilized for the obtained data and also the verification portion of the study will be explained. Continuing, detailed single cutter integration and bit performance parameters that proved key to the development of the PDC drill bit model shown in this study are provided. Lastly, the obtained lab data will be shown and applied to two separate calibration approaches for the PDC drill bit model developed in this study.

3.1 Single Cutter Modeling

Single cutter modeling is often times used in the evaluation of PDC single cutter performance. Detailed models described in section 2.1 show not only general normal and drag forces are accounted for in these studies but also other parameters such as novelty PDC designs, chamfer

forces, cutting evacuation forces, and the frictional forces needed to be overcome for accurate single cutter modeling. Single cutter modeling is the corner stone in this study that allowed for further understanding of single cutter performance. With that, single cutter modeling could be integrated in the development a full hole PDC drill bit ROP model explained in this chapter.

3.1.1 Single Cutter Testing

Single cutter experimental data from multiple sources were collected for evaluation. The data obtained were the results reported from testing conducted on a VTL with unsaturated test samples varying in lithology under atmospheric conditions. Testing conducted on a VTL begins along circumference of the rock sample and the cutter is plunged into the rock. Once this occurs, the VTL begins to operate in a cylindrical path where the radius of the operating point nears the center of the testing sample. This ensures that the cutter being evaluated is exposed to virgin rock over the course of an entire test run. Aside from the publicly obtainable data shown in these studies, additional third party single cutter testing is incorporated within the analysis and will be denoted as “OSU data”.

3.1.2 Contact Area between Rock & PDC Cutter

When incorporating a physical single cutter force model, the main variable needed to be accurately estimated is the contact area at the interface of the rock and cutter. Taking the area of a circle and using common geometric principles to describe rock/cutter contact area (A_C) can then be described as below in Equation 3.1 and Equation 3.2.

$$A_C = (\frac{D_c}{2})^2 * Cos^{-1}\left(\frac{\frac{D_c}{2}*h}{\frac{D_c}{2}}\right) - (\frac{D_c}{2} - h)*(2*\left(\frac{D_c}{2}\right) * h - (h)^2) \quad (3.1)$$

D_c: Cutter diameter (in)

h: Primary depth of cut experienced by the cutter due to back rake (in)

Equation 3.2 is used to estimate the DOC associated to the area of rock/cutter contact that is generating the normal and drag forces.

$$h = \frac{\delta}{Cos(\theta)} \tag{3.2}$$

δ: Depth of cut (in)

θ: Back rake angle (degree)

3.1.3 Single Cutter Force Modeling

The single cutter force model that was adopted for this study was developed by (Detournay and Defourny, 1992). The sharp single cutter force model explained in section 2.1 is shown by Equations 3.3 and 3.4.

$$F_d = \varepsilon * A_c \tag{3.3}$$

$$F_n = \zeta * \varepsilon * A_c \tag{3.4}$$

Where:

F_n: Normal force (lbf)

F_d: Drag force (lbf)

A_c: Rock/cutter contact area (in^2)

ζ: Ratio of normal and drag forces (-)

ε: Intrinsic specific energy ($\mathrm{lb/in^2}$)

For perfectly sharp cutters these become: $\varepsilon = E$ and $\mathrm{S} = \zeta * \varepsilon$ (3.5) and (3.6)

E: Specific energy ($\mathrm{lb/in^2}$)

S: Drilling strength ($\mathrm{lb/in^2}$)

$$\zeta = \frac{E}{S} = \frac{\frac{F_n}{A_c}}{\frac{F_d}{A_c}} = \frac{F_n}{F_d} = \tan(\theta + \psi) \quad (3.7)$$

θ: Cutter back rake angle (degree)

ψ: Interfacial friction angle (degree)

The sharp cutter force balance for the Detournay and Defourny (1992) model is shown in Figure 3.1.

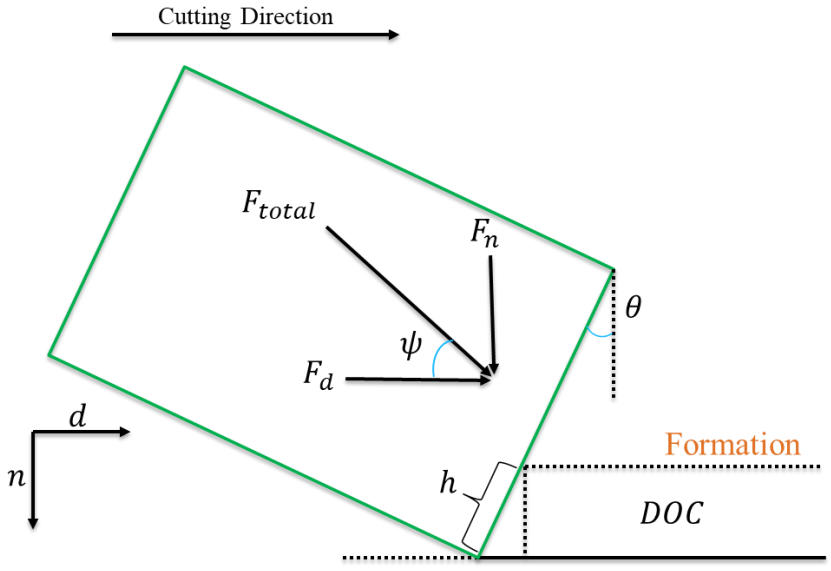

Figure 3.1: Schematic of sharp cutter force model

3.2 Interfacial Friction Angle

Interfacial friction angle (IFA) reported in Detournay and Defourny (1992) is used to explain frictional effects experienced at the cutting face. For single cutter testing, Equation 3.8 is used to calculate single cutter IFA (ψ) from experimental data. Performance of single cutter testing is generally over estimated in hard rock if IFA is not taken into account.

$$\psi = \tan^{-1}\left(\frac{F_n}{F_d}\right) - BR \tag{3.8}$$

BR: Back rake angle (degree)

3.2.1 Effects of Depth of Cut on Interfacial Friction

From experimental data shown in Table A-1 were obtained from Glowka (1987). Additional data reported in Hellvik et al. (2012) were obtained from their study which evaluated the effects back rake on normal and drag forces. Using these two data sets, an analysis of DOC and its impact on IFA was taken up. It was found that at an optimal DOC, IFA tends to become a constant value. The evaluation of the Hellvik et al. (2012) data in Texas Pink Granite is shown in Figure 3.2 and similarly the evaluation of the Glowka (1987) data shown in Table A-1 in Sierra white Granite is shown in Figure 3.3.

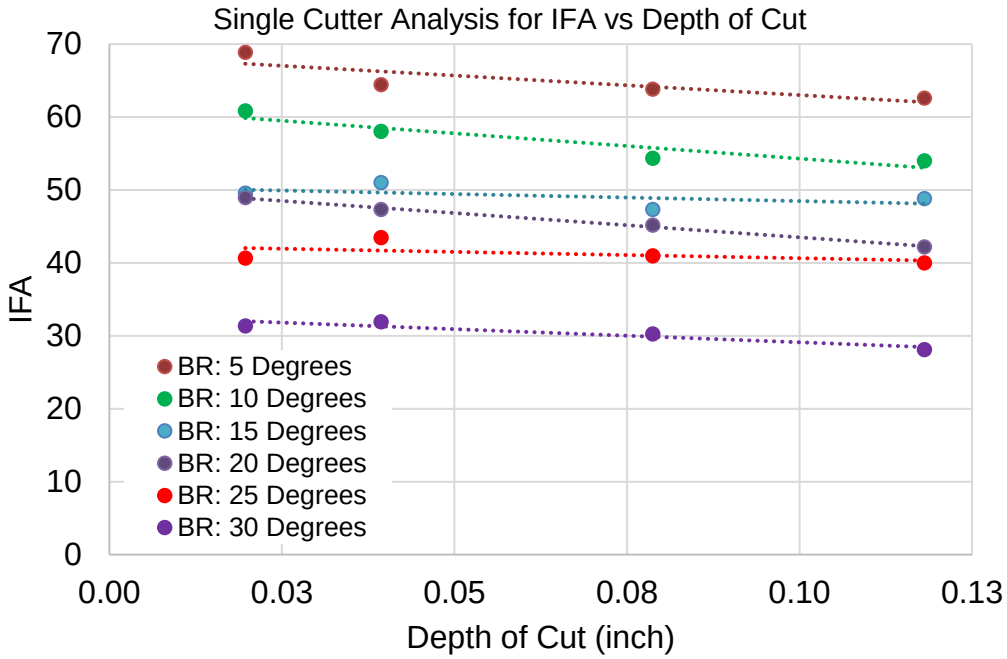

Figure 3.2: IFA vs. DOC for Texas Pink Granite (Hellvik et al. 2012)

As seen above from Figure 3.2, for all back rake values, after a DOC of roughly 0.04 inches was achieved IFA began to remain relatively constant.

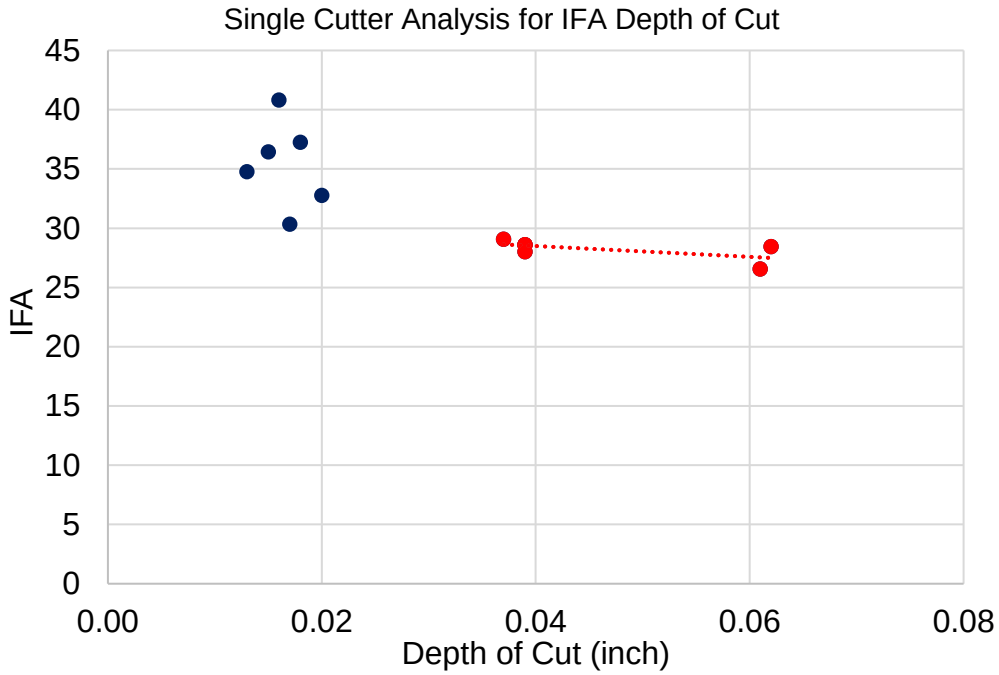

Figure 3.3: IFA vs. DOC for Sierra White Granite (OSU data)

Figure 3.3 shows inefficient cutting data points in blue and efficient cutting due to optimal DOC in red data points. Similar to the Texas Pink Granite evaluation, constant IFA is achieved at roughly 0.04 inch DOC. After confirming that IFA is a constant after optimal DOC is achieved, frictional effects associated to the cutter can be utilized in the development of the hard rock ROP model.

3.2.2 Effects of Back Rake on Interfacial Friction

Additional studies were carried out on the Hellvik et al. (2012) and third party OSU data were conducted to analyze the effects of back rake and the influences it holds on single cutter force modeling. The studies analyzed for this testing used similar PDC cutter design but were tested on two different lithologies. The data for rock strength, cutter test velocity, and diameter of cutter are

shown in Table 3.1. The findings for the two different lithologies, as seen in Figure 3.4, show similar trends in IFA for different back rake angles.

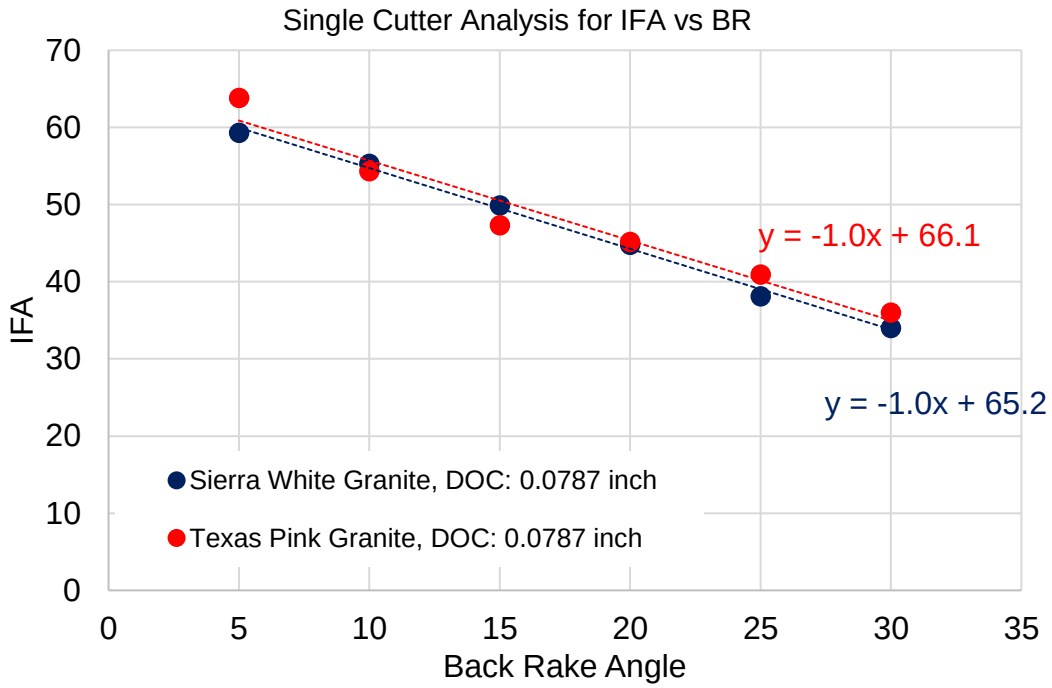

Figure 3.4: IFA vs. Back Rake for Texas Pink & Sierra White Granite

The findings indicate that for the single cutter testing analyzed, IFA appears to be a function independent of back rake.

3.2.3 Effects of Wear on Interfacial Friction

Wear on a PDC cutters play a role in evaluating IFA. As wear increases, the wearflat area begins to increase allowing for more surface area to be in contact with the formation. Using data obtained from Hellvik et al. (2012) it is confirmed analytically, as shown in Figure 3.5, that IFA increases as wear increases on a PDC cutter. These tests were conducted on Texas Pink Granite and Torrey Bluff Sandstone rock samples where data for rock strength, cutter test velocity, and diameter of cutter is shown in Table 3.1. This study was conducted to measure the performance of

PDC cutters with varying wear. The test set up for this evaluation implemented 30 minute testing intervals at 0.12 inch DOC. Following each test, the PDC cutters were then labeled with a wear state reference nominalized as “P-val”, where the P-val is the number of 30 minute tests using the same cutter increasing cutter wear with number of tests.

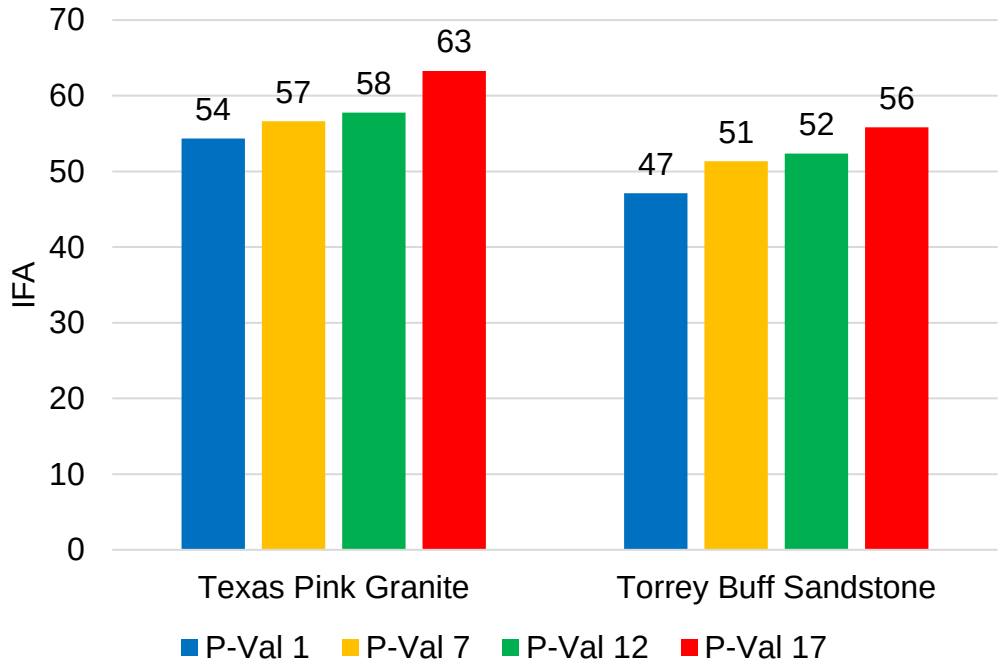

Figure 3.5: Impact of wear on IFA (Hellvik et al. 2012)

Test Study	Rock Type	Rock Strength [psi]	Linear Velocity [inch/sec]	Dc [inch]
Glowka 1987	Sierra White Granite	21,500	2.2	0.5
Hellvik et al. 2012	Texas Pink Granite	19,317	133.9	0.63
Hellvik et al. 2012	Torrey Bluff Sandstone	8,993	133.9	0.63
OSU Data	Sierra White Granite	21,013	98.4	0.63

Table 3.1: Data for single cutter test parameters and reported rock strengths

3.3 Development of New PDC Drill Bit ROP Model

Once the single cutter testing and analysis was complete, the task of developing a newly integrated PDC drill bit ROP model for hard rock was then taken up. It was key that the model used data readily found in the field or lab so that the integration into the larger real time drilling optimization system would be possible.

3.3.1 Test Facility

Much like single cutter testing facilities, full hole testing is often conducted in laboratories to better understand performance under controlled environments. The full hole testing conducted at SNL uses what is known as the Hard Rock Drilling Facility (HRDF) which is shown in Figure 3.6. This system was developed to reproduce dynamic properties of a deep drill string under field like operations. The results shown in the following studies were conducted with a rigid drilling assembly, no confining pressures and water as the drilling fluid.

Figure 3.6: SNL Hard Rock Drilling Facility (Raymond et al. 2015)

3.3.2 Single Cutter and Bit Performance Integration

The model developed in this study shown by Equation 3.9 and Equation 3.10 incorporates variations to the Kerkar et al. (2014) PDC drill bit ROP model. The variations create a model that is better suited to estimate penetration rates based on PDC single cutter performance. The PDC drill bit geometry coefficient (G) shown by Equation 3.9 was used to incorporate parameters associated to cutters being implemented as well as the physical design of the bit.

$$G = k1 * \left(\frac{N_B * D_c * cos(SR)}{N_c * (D_B * f_B(D_B)) * tan(\psi + BR)}\right) \tag{3.9}$$

Where:

N_B: Number of blades (-)

D_c: Cutter diameter (in)

N_c: Number of Cutters (-)

D_B: Bit diameter (in)

$f_B(D_B)$: Bit diameter efficiency function

ψ: Interfacial friction angle (degree)

BR: Cutter back rake (degree)

SR: Cutter side rake (degree)

k_1: Bit performance empirical coefficient

$$ROP = G * \frac{WOB^{a1} * RPM^{b1}}{UCS^{c1}} * w(f) * h(x) \tag{3.10}$$

Where:

ROP: Rate of penetration (ft/hr)

WOB: Weight on bit (klbf)

RPM: Rotary speed of bit (Revolution/min)

UCS: Unconfined compressive strength ($\mathrm{lb/in^2}$)

$w(f)$: Cutter wear function (-)

$h(x)$: Hydraulic efficiency function (-)

a_1, b_1, c_1: Drilling performance in varying lithology empirical coefficients

Incorporating the number of primary cutters (N_c) allows for an efficiency of weight distribution to be accounted for over the total number of cutting structures on the face of the bit. Since WOB is now in terms of single cutter efficiency, using similar principles found in Detournay and Defourny (1992) that are used to estimate IFA for single cutter testing, it can then be extrapolated into a full hole expression. Moreover, single cutter IFA estimations incorporate the ratio of the normal and drag forces which becomes the primary parameter needed to calculate IFA. To do this for a full hole estimation, parameters need to be broken down into single cutter expressions. To accomplish this, the normal force becomes weight on cutter (WOC) and drag force becomes torque on cutter (TOC) Using these common parameters recorded in experimental drilling data the correlation to estimate full hole IFA is shown in Equation 3.11.

$$\psi = \tan^{-1}\left(\frac{WOC}{TOC}\right) - BR \tag{3.11}$$

Where:

ψ: Interfacial friction angle (degree)

WOC: Weight on cutter (klbf)

TOC: Torque on cutter (ft $*$ klbf)

BR: Cutter back rake angle (degree)

To find WOC and TOC parameters needed outside of testing data are able to be found within bit specification sheets. In addition, these parameters being readily available would allow these expressions to be monitored with real time data in the field or lab testing.

$$WOC = \frac{WOB}{N_c} \tag{3.12}$$

$$TOC = \frac{\frac{Torque}{Re}}{N_c} \tag{3.13}$$

$$Re = \frac{D_B}{2*\sqrt{2}} \tag{3.14}$$

Where:

N_c: Number of primary cutters (-)

Re: Equivalent radius (in)

D_B: Bit diameter (in)

In addition, the bit diameter efficiency function ($f_B(D_B)$) accounts for bit performance generally seen within field application. As indicated by Mensa and Martyn (2001), penetration rates do not always improve as bit diameter is reduced. Moreover, decreasing bit diameter after a point reduces penetration rates if all other operating parameters are held constant. Laboratory and field results indicated by Warren (1981) claim maximum bit performance is seen out of 8.5 inch bits. The efficiency function shown by Equation 3.15 is empirically calibrated using normalized ROP values from data recorded by Warren (1981) where similar borehole conditions were used. The empirical values found to maximize ROP when the input bit diameter is 8.5 inches is shown in Table 3.2.

$$f_B(D_B) = r_1 * D_B^4 + r_2 * D_B^3 + r_3 * D_B^2 + r_4 * D_B + r_5 \tag{3.15}$$

D_B: Bit diameter (in)

r_1, r_2, r_3, r_4, r_5: Empirically calibrated constants

Empirical Constants	Value
r1	106.4
r2	-33.3
r3	-34.6
r4	14.4
r5	-0.4

Table 3.2: Empirical constants for bit diameter efficiency function

A visual representation of how the bit diameter efficiency function is distributed for bit sizes ranging from 3.75 to 17.5 inches is shown by Figure 3.7.

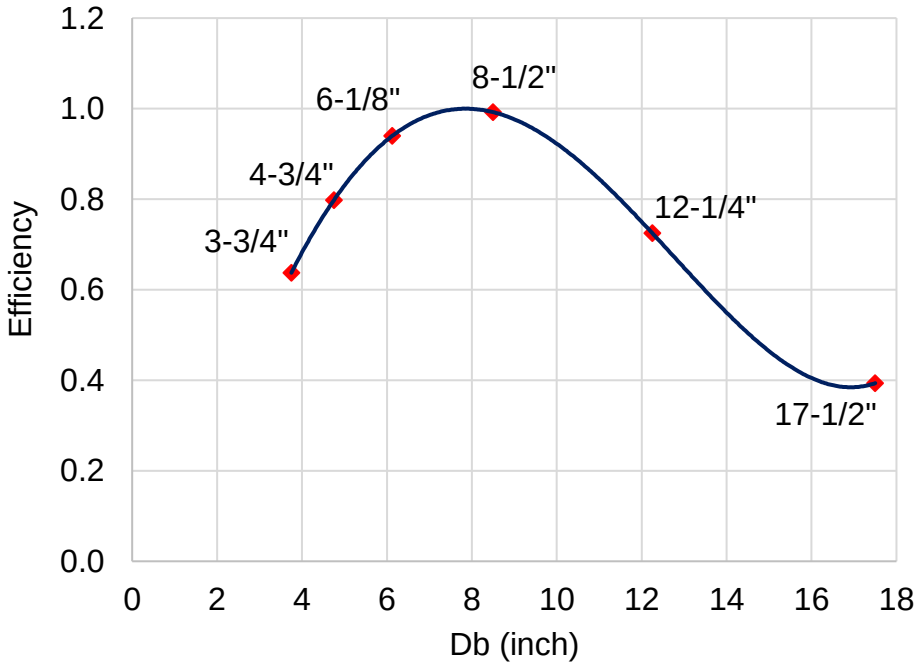

Figure 3.7: Bit diameter efficiency distribution

Using the findings in section 3.2, after an optimal DOC is achieved, IFA becomes more or less a constant parameter as shown in Figures 3.3 and 3.4. It has been estimated that once IFA becomes constant, it remains roughly the same for optimal drilling operating ranges for full hole application. This optimal drilling range is known as phase II or where WOB and ROP share a linear relationship. Before this optimal range is achieved, phase I is the dominating phase which is explained as the effects of inefficient drilling due to limited DOC. Moreover, once the optimal range is exceeded this is considered phase III, or the flounder point. Once the flounder point is achieved effects of inefficient cutting are potentially caused due to regrinding of cuttings and/or inefficient hydraulics. A representation of these three phases of drilling can be found in Figure 3.8.

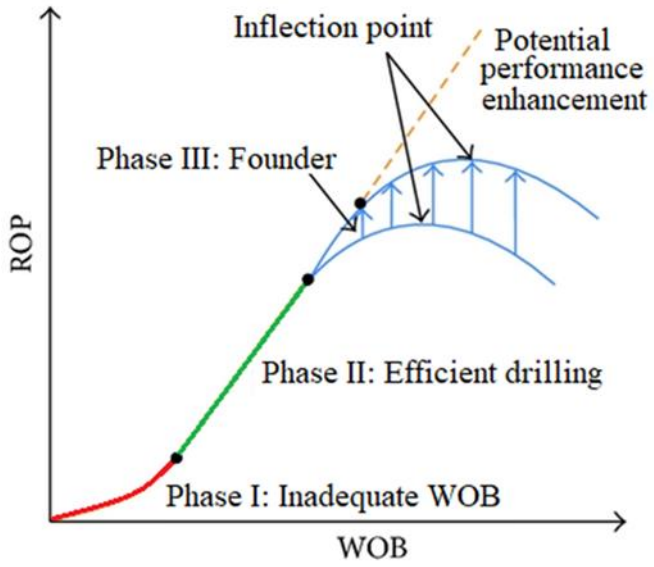

Figure 3.8: ROP vs. WOB (Three identifiable phases of drilling)

3.3.3 New PDC Drill Bit ROP Model Calibration

The constants for the developed ROP model in this study were found using full hole data recorded by Raymond et al. (2015). The data sets used from the Raymond et al. (2015) study

were for two 3.75 inch PDC bits, one being a 4 blade and the other a one 5 blade. The PDC bits were run at RPM values of 100 and 150. The tests were conducted in a hard granite lithology known as Sierra White Granite. The 4 and 5 bladed PDC bits used are shown in Figure 3.9 and Figure 3.10 which were tested at SNL specifications and manufactured from Ulterra Drilling Technologies.

Figure 3.9: Ulterra 3.75 inch 4 blade (Raymond et al. 2015)

Figure 3.10: Ulterra 3.75 inch 5 blade (Raymond et al. 2015)

From there, two approaches were taken up to calibrate the model shown by Equations 3.9 and 3.10. For approach one, empirically calibrating the constants (K_1) (a_1) (b_1), and $(c_1)$was conducted by reducing the overall estimated ROP deviation as shown by Equation 3.16 and trend

analysis. Approach one only incorporated data from the phase II (i.e. WOB greater than 2,000 lbs) data points shown in Table A-2 and used a constant IFA value of 41 degrees.

$$Average\ ROP\ Deviation = \frac{\sum(|ROP_{data} - ROP_{model}|)}{number\ of\ data\ points} \quad (3.16)$$

In the second approach, implemented a Differential Evolution Algorithm (DEA) which was applied to estimate the best fit for the empirical constants (K_1) (a_1) (b_1), and (c_1) using the same data set as approach one.

The results for approach one model calibration is provided in Equation 3.16 and 3.17.

$$G = 0.000061 * \left(\frac{N_B * D_c * cos(SR)}{N_c * (D_B * f_B(D_B)) * tan(\psi + BR)}\right) \quad (3.16)$$

$$ROP = G * \frac{WOB^{2.7} * RPM^{0.7}}{UCS^1} * w(f) * h(x) \quad (3.17)$$

The model fitting results are shown below in Figures 3.11 through 3.15.

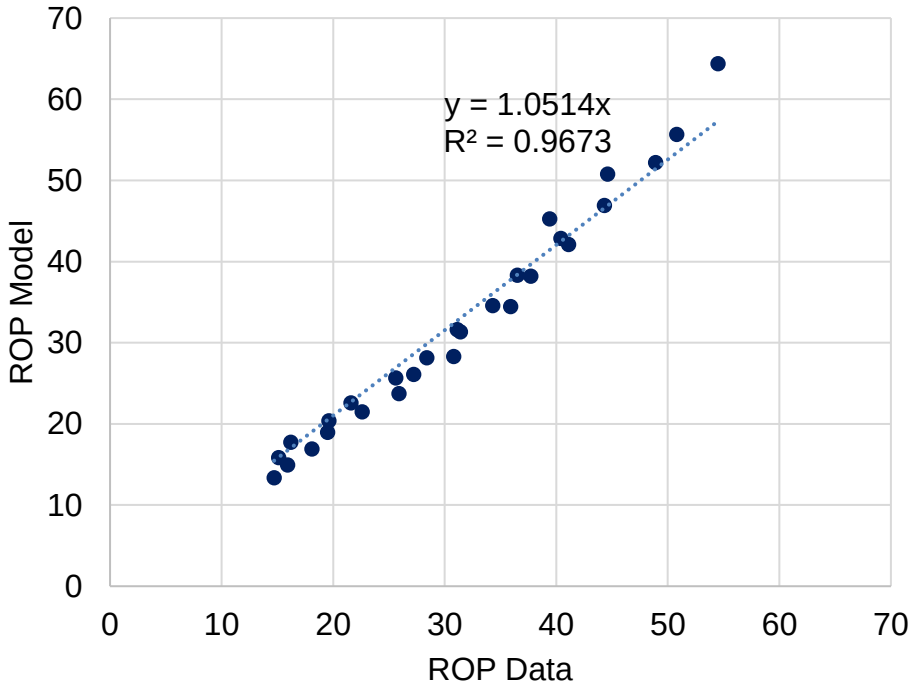

Figure 3.11: Comparison between approach one model estimated ROP and data (Raymond et al. 2015)

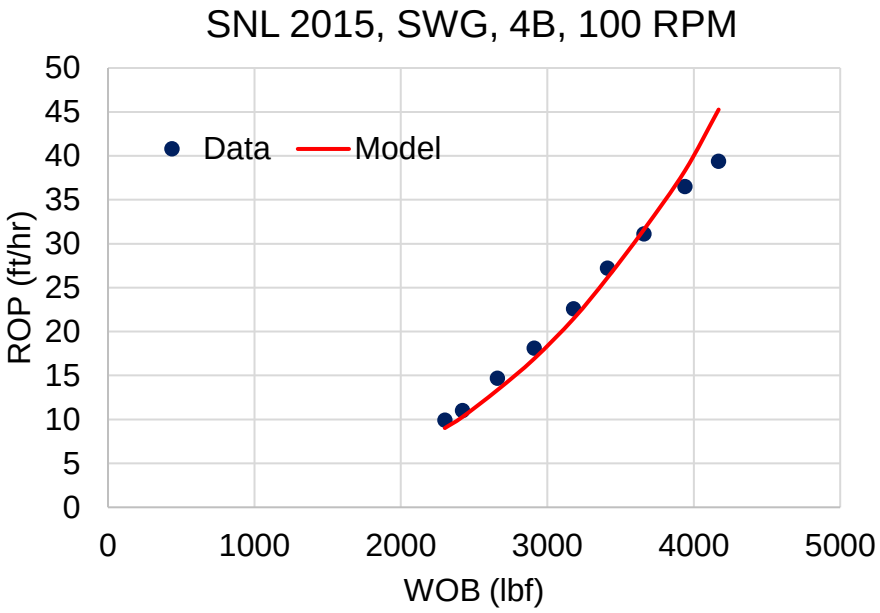

Figure 3.12: Comparison between approach one model estimated ROP and data for 4 bladed PDC bit at 100 RPM in SWG (Raymond et al. 2015)

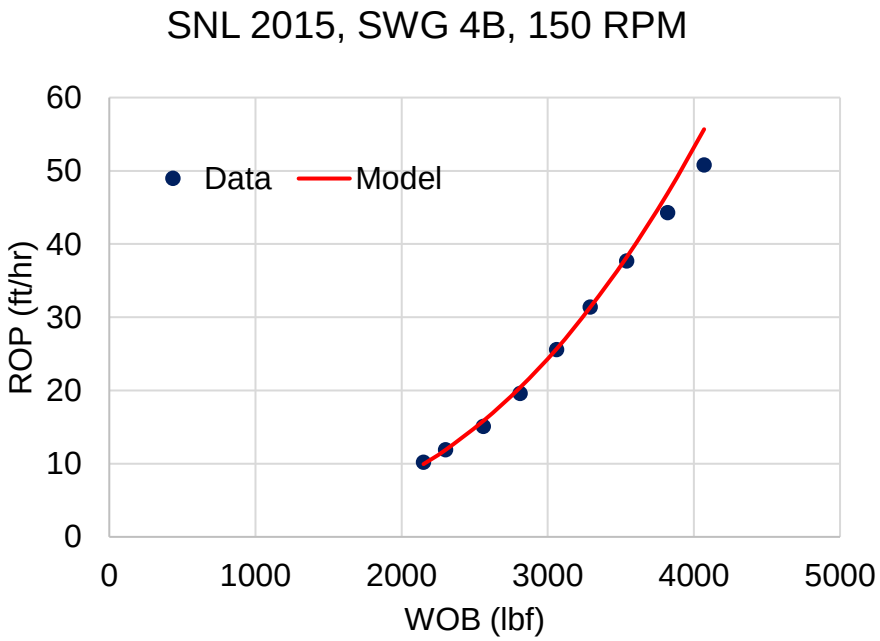

Figure 3.13: Comparison between approach one model estimated ROP and data for 4 bladed PDC bit at 150 RPM in SWG (Raymond et al. 2015)

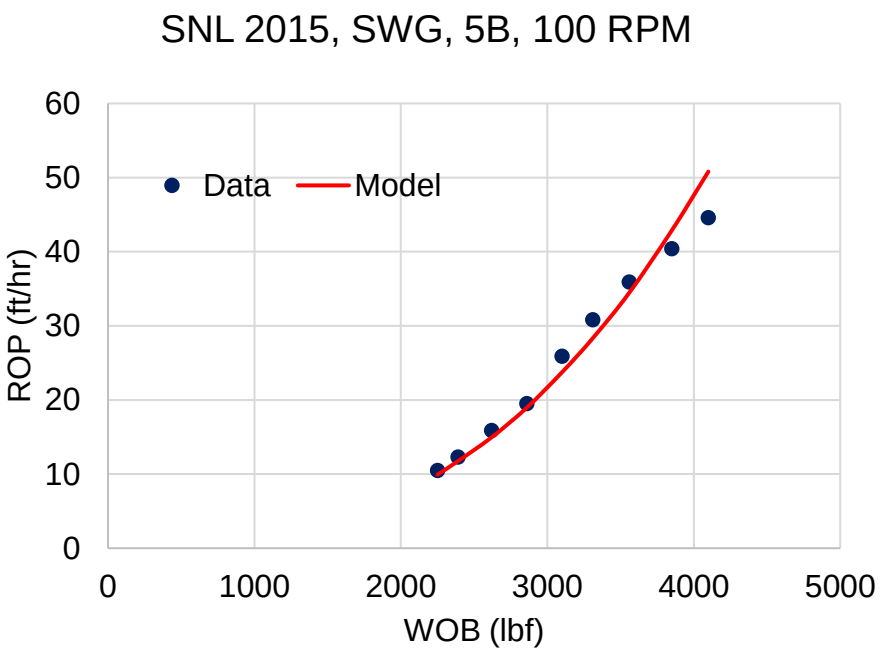

Figure 3.14: Comparison between approach one model estimated ROP and data for 5 bladed PDC bit at 100 RPM in SWG (Raymond et al. 2015)

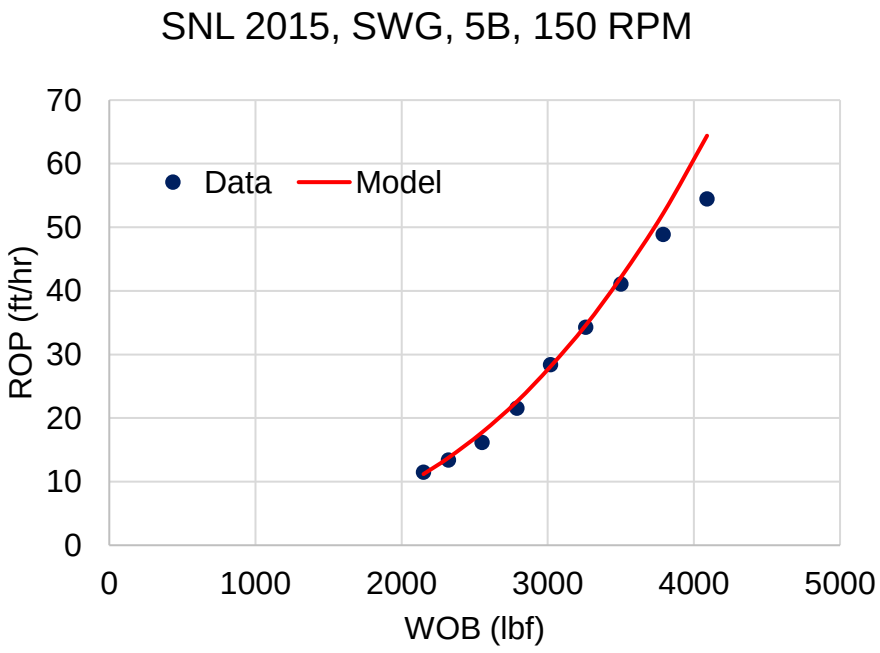

Figure 3.15: Comparison between approach one model estimated ROP and data for 5 bladed PDC bit at 150 RPM in SWG (Raymond et al. 2015)

The results for the second approach model calibration are provided in Equation 3.18 and 3.19.

$$G = 0.0008 * \left(\frac{N_B * D_c * cos(SR)}{N_c * (D_B * f_B(D_B)) * tan(\psi + BR)}\right) \tag{3.18}$$

$$ROP = G * \frac{WOB^{2.451} * RPM^{0.566}}{UCS^{0.986}} * w(f) * h(x) \tag{3.19}$$

The model fitting results are shown below in Figures 3.16 through 3.20.

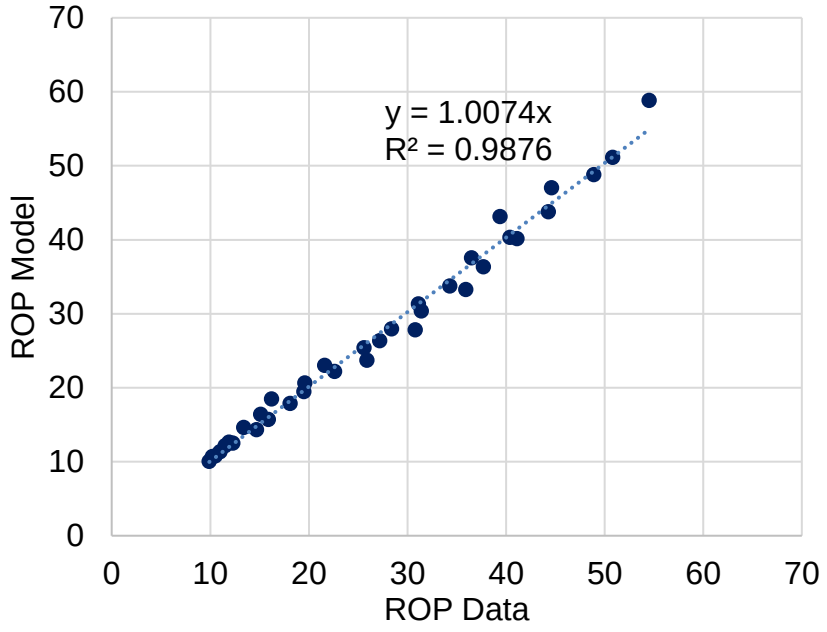

Figure 3.16: Comparison between approach two model estimated ROP and data (Raymond et al. 2015)

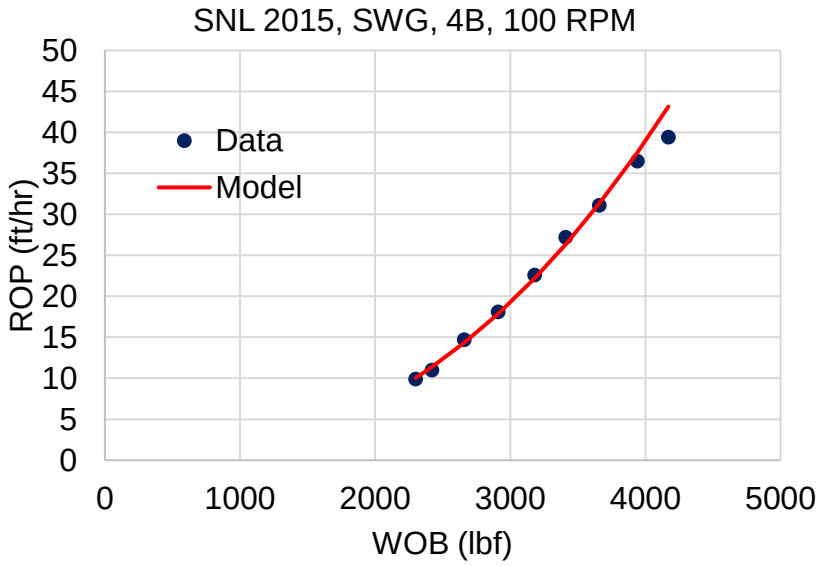

Figure 3.17: Comparison between approach two model estimated ROP and data for 4 bladed PDC bit at 100 RPM in SWG (Raymond et al. 2015)

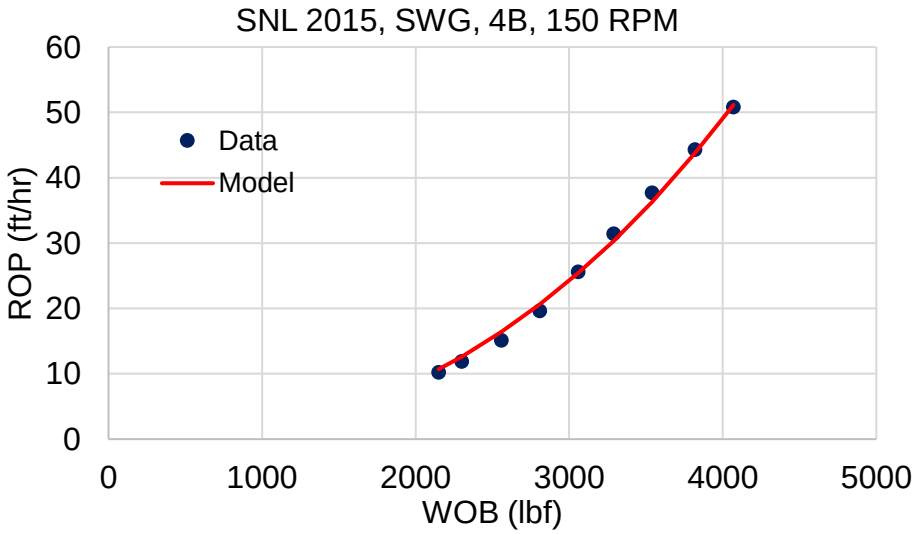

Figure 3.18: Comparison between approach two model estimated ROP and data for 4 bladed PDC bit at 150 RPM in SWG (Raymond et al. 2015)

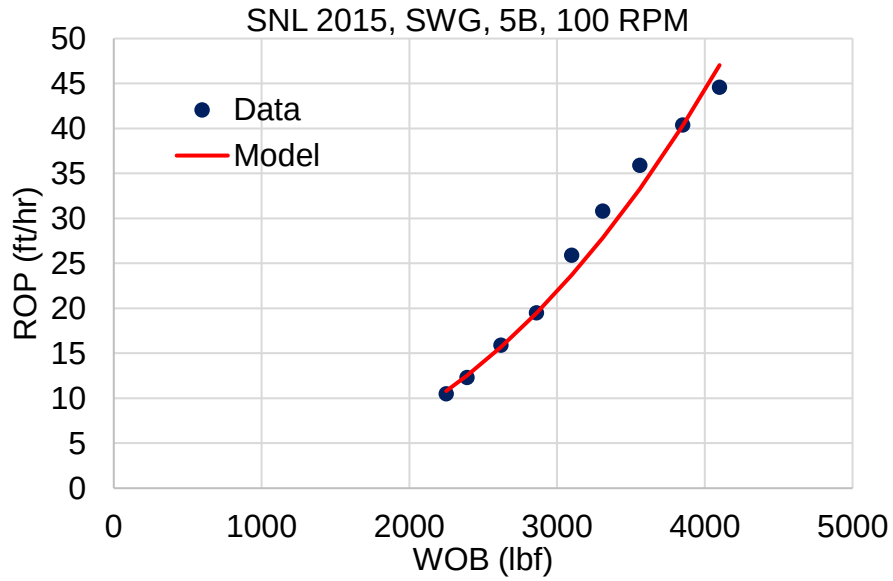

Figure 3.19: Comparison between approach two model estimated ROP and data for 5 bladed PDC bit at 100 RPM in SWG (Raymond et al. 2015)

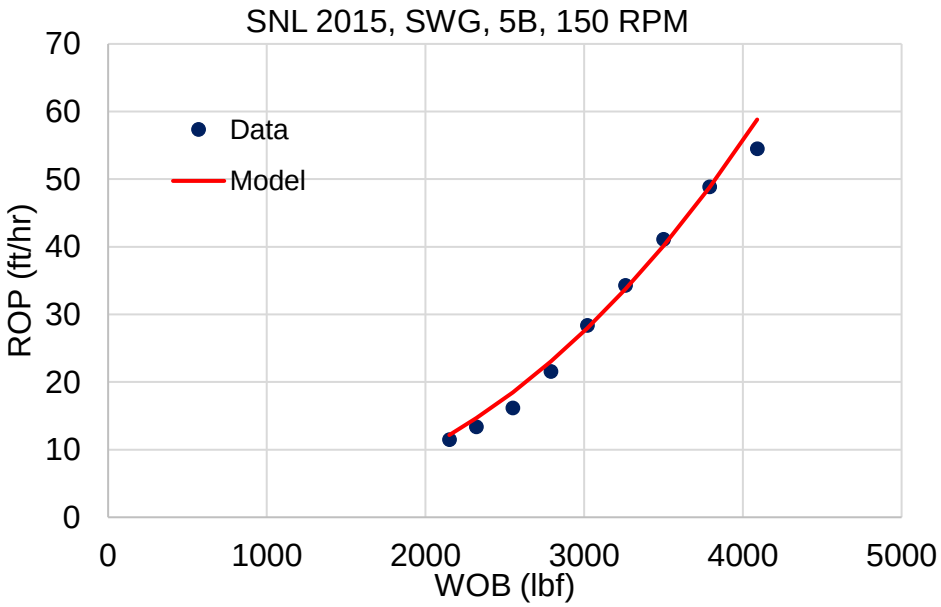

Figure 3.20: Comparison between approach two model estimated ROP and data for 5 bladed PDC bit at 150 RPM in SWG (Raymond et al. 2015)

Both approaches showed a good match when being compared to the calculated ROP for the model against the 2015 SNL laboratory data. Though both showed good matches, approach two showed to be the more accurate model upon completion of the calibration process. Approach one, as shown in Figure 3.11, displayed a 5 percent mismatch between the model and the laboratory data at higher ROP. It is assumed that the lab data deviates from the trend at higher ROP values due to hydraulics. This discrepancy was considered in the WOB vs ROP trend analysis to obtain the coefficients for the model.

3.4 Hydraulic Inefficiency Component

The equation shown by Equation 3.20 is used to estimate hydraulic inefficiencies from the ROP model developed by Kerkar et al. (2014). The empirically calibrated constants$(a2)$, $(b2)$, and $(c2)$ are shown in Table 3.3

$$h(x) = a2 * \frac{(HSI * \frac{JSA}{2 * D_B})^{b2}}{ROP^{c2}} \tag{3.20}$$

HSI: Hydraulic performance of the bit $(\mathrm{hp/in^2})$

JSA: Junk slot area $(\mathrm{in^2})$

D_B: Bit diameter (in)

ROP: Rate of penetration based off perfect cleaning conditions $(\mathrm{ft/hr})$

a_2, b_2, c_2: Hydraulic empirical coefficients

Empirical Constants	Value
a2	10.5
b2	0.55
c2	0.5

Table 3.3: Empirical constants for hydraulic efficiency function

Figure 3.21 is a graphical representation of how hydraulic inefficiencies impact penetration rates if not optimized.

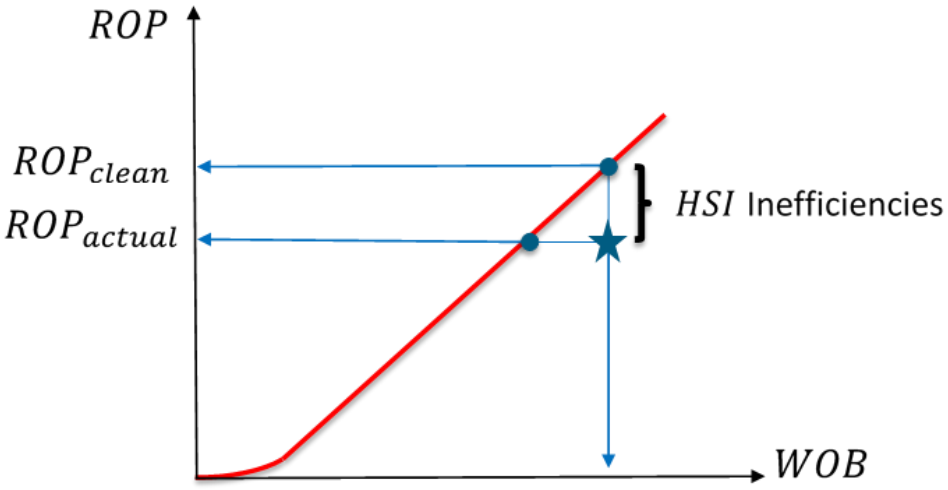

Figure 3.21: HSI effects on penetration rates

Using data obtained from third party testing, Figure 3.22 shows how the hydraulic model was calibrated for this study.

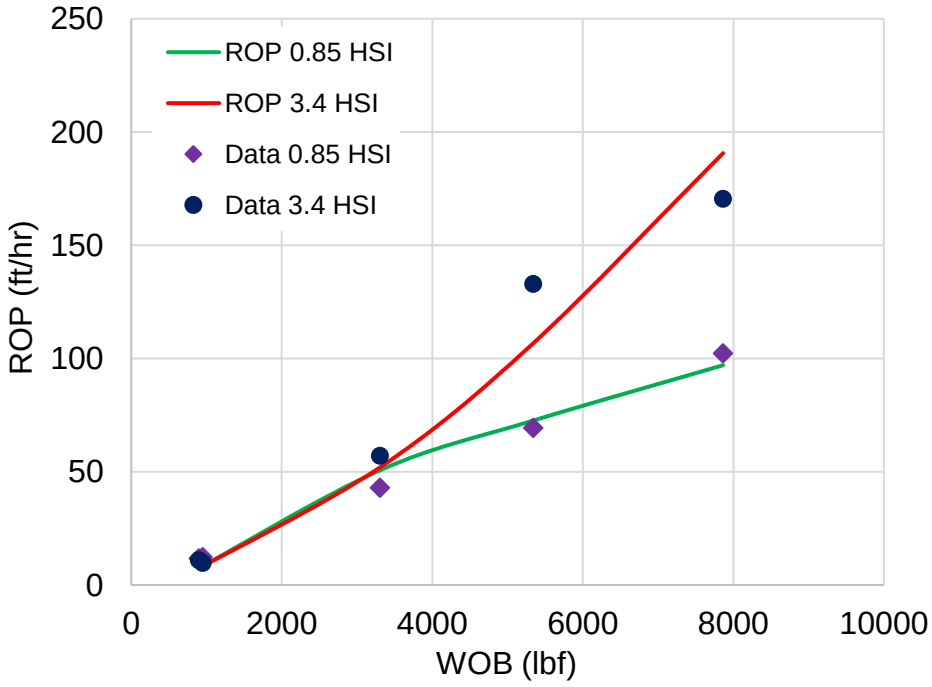

Figure 3.22: Hydraulic model calibration (OSU data)

As it can be seen in Figure 3.23 as hydraulic efficiency is increased, higher rates of penetration are able to be achieved.

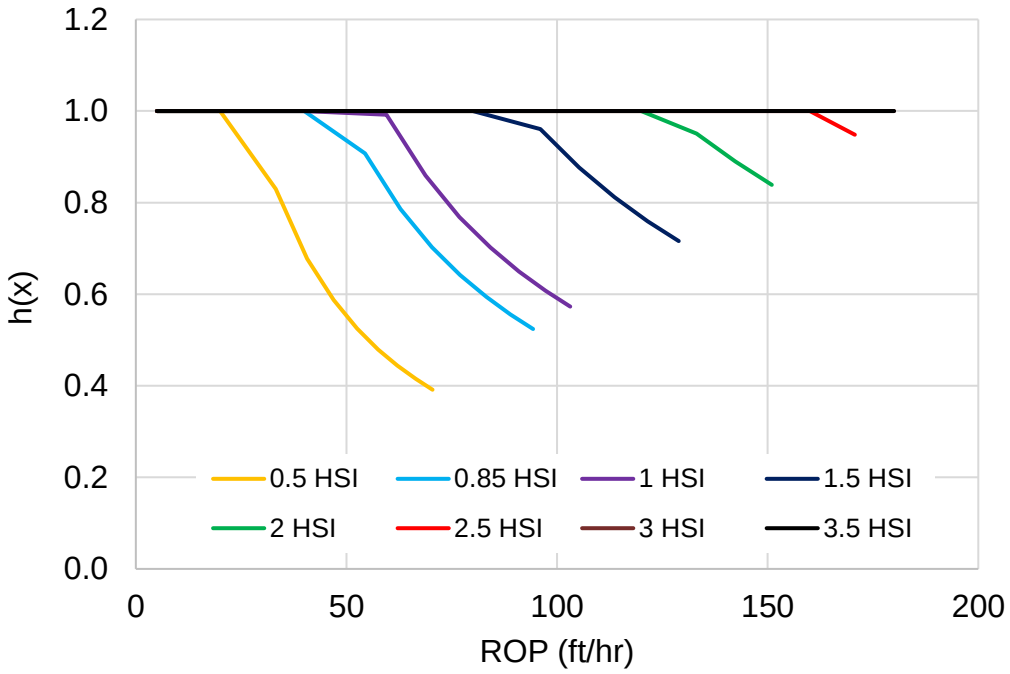

Figure 3.23: Penetration rate performance with increasing HIS (OSU data)

A schematic was created to visually summarize the progression of the ROP model developed in this study which can be seen in Figure 3.24.

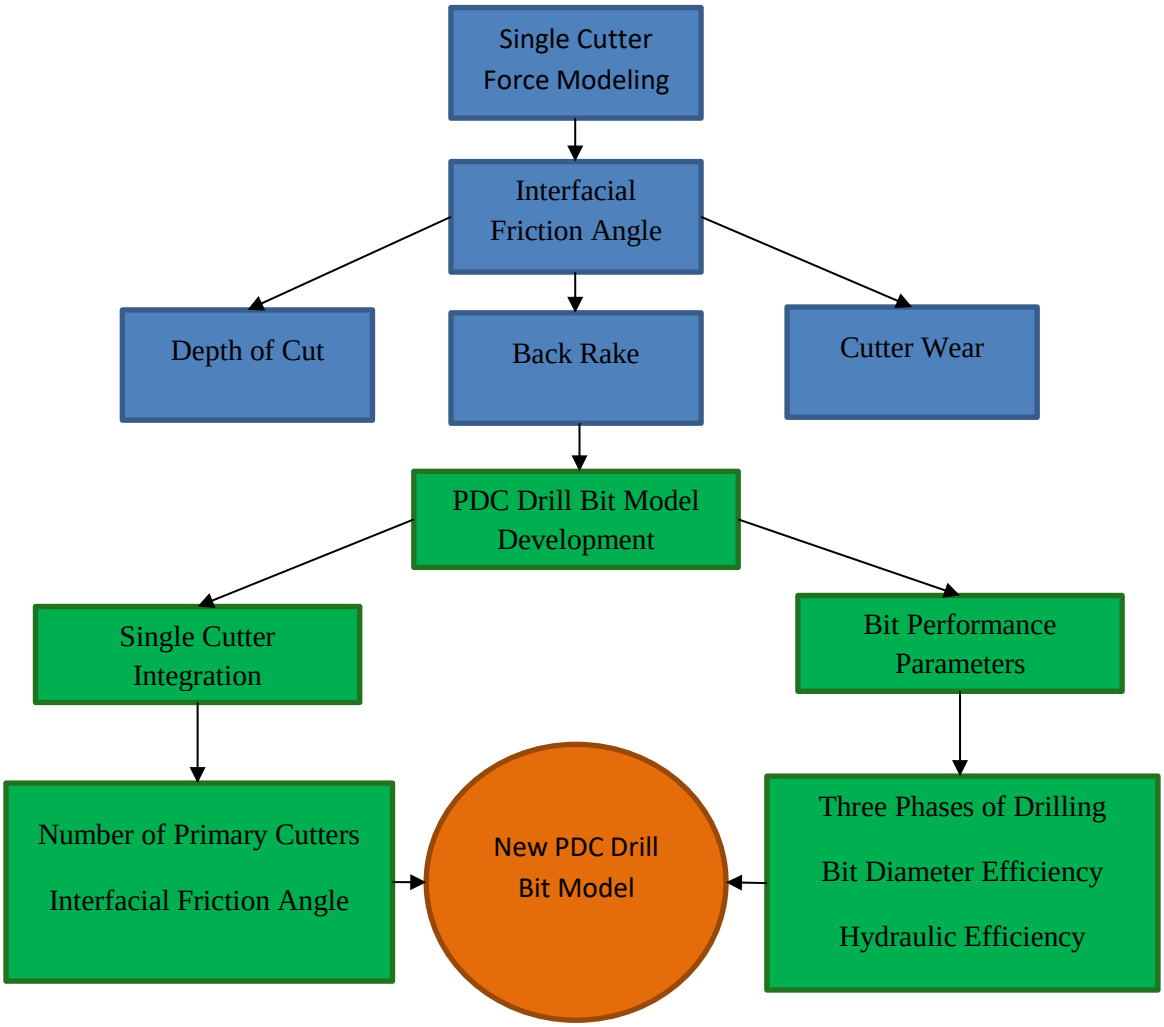

Figure 3.24: Flow chart of model progression

CHAPTER IV

DATA ANALYSIS

This chapter provides the verification process of the new single cutter based PDC drill bit ROP model by applying both calibrated model approaches to new full hole data. The new full hole data (NOV 2019) was obtained through testing conducted at Sandia National Laboratories (SNL) which was conducted in conjunction to the development of the PDC drill bit ROP model developed in this study. This testing implemented a similar test set up to the studies conducted by Raymond et al. (2015), where 3.75 inch 4 and 5 bladed PDC bits at varying RPM values were incorporated to analyze drilling performance in hard rock.

4.1 Verification of Full Hole Interfacial Friction Angle

As can be seen in Figure 4.1 the IFA using full hole drilling data in Phase II is represented by two green data points. The data point at 15 degrees back rake was drilled with the 4 bladed Ulterra bit used in Raymond et al. (2015) and the data point at 25 degrees back rake was drilled with the 4 bladed NOV bit (NOV 2019). Each of the data points is the average IFA in Phase II calculated

from multiple data points using the bit WOC, TOC and the equivalent radius concept. The full hole IFA findings were then compared to single cutter testing found in Section 3.2.2. When comparing the difference in the single cutter and full hole IFA there appears to be a reduced correlation in the full hole data to that of the single cutter data. This is potentially due to the overlap of the cutting profiles of a full hole bit compared to a single cutter cutting action. Another explanation could be the difference in PDC cutter chamfers since the single cutter data had 45 degree chamfer while the full hole bits did not. Therefore, with a full hole bit, the cutter potentially sees a lesser area in front of the cutter due to the cutter overlap and chamfer sizes. Another possible difference is that in the IFA full hole calculation incorporates an equivalent cutter radius and number of PDC cutters for the drill bit to estimate the cutter horizontal force from the bit torque. Another, key observation from the full hole data is that as the back rake increases 10 degrees, the IFA decreases 10 degrees. This means during the Phase II operating range the combined BR+IFA is a constant.

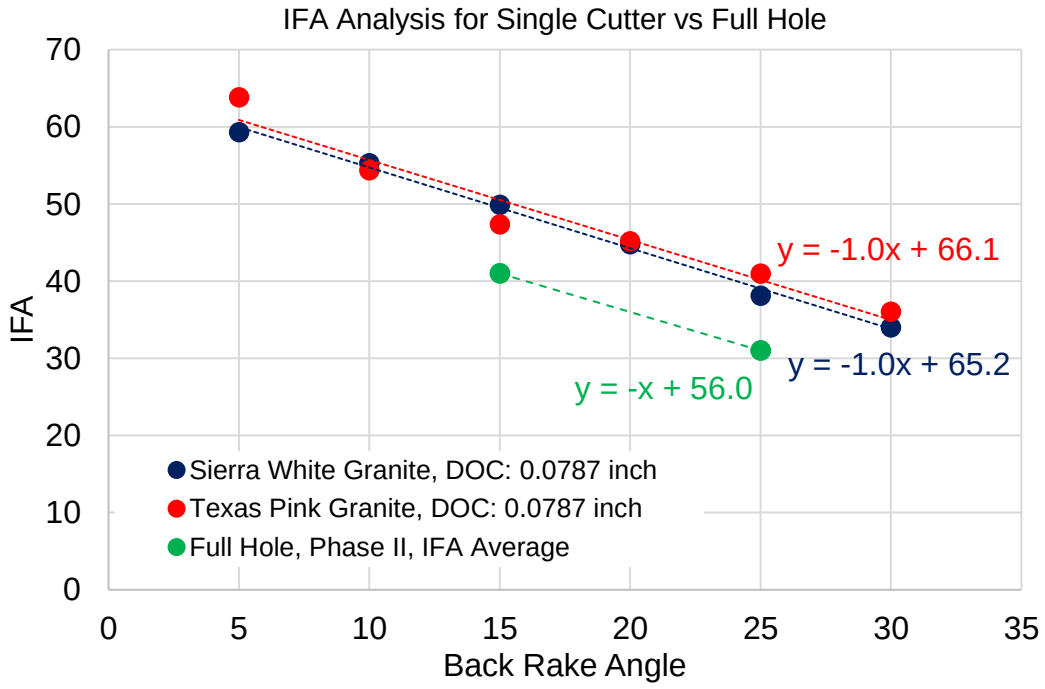

Figure 4.1: IFA Analysis for Single Cutter vs. Full Hole

Test Study	Rock Type	Rock Strength [psi]	Linear Velocity [inch/sec]	Dc [inch]
Glowka 1987	Sierra White Granite	21,500	2.2	0.5
Hellvik et al. 2012	Texas Pink Granite	19,317	133.9	0.63
Hellvik et al. 2012	Torrey Bluff Sandstone	8,993	133.9	0.63
OSU Data	Sierra White Granite	21,013	98.4	0.63
Raymond et al. 2015	Sierra White Granite	26,000	13.9 - 20.8	0.43
NOV 2019	Sierra White Granite	26,000	11.1 - 16.7	0.43

Table 4.1: Data for single cutter and full hole test parameters and reported rock strength

4.2 Verification of the New PDC Drill Bit ROP Model

The NOV 2019 data set incorporated two 3.75 inch PDC drill bits shown in Figure 4.2 and Figure 4.3 one being a 4 blade and the other a 5 blade. The new PDC drill bits used were designed to specifications requested by the OSU research team then purchased from NOV. The NOV 2019 data shown in Table A-3 was then compared to the calibrated model which incorporated results from Raymond et al. (2015).

Figure 4.2: NOV 3.75 inch 4 blade (NOV 2019)

Figure 4.3: NOV 3.75 inch 5 blade (NOV 2019)

The testing performed at SNL for the NOV 2019 data set was conducted at RPM values of 80, 120 and 160. The results of the approach one are seen in Figures 4.4 through 4.10.

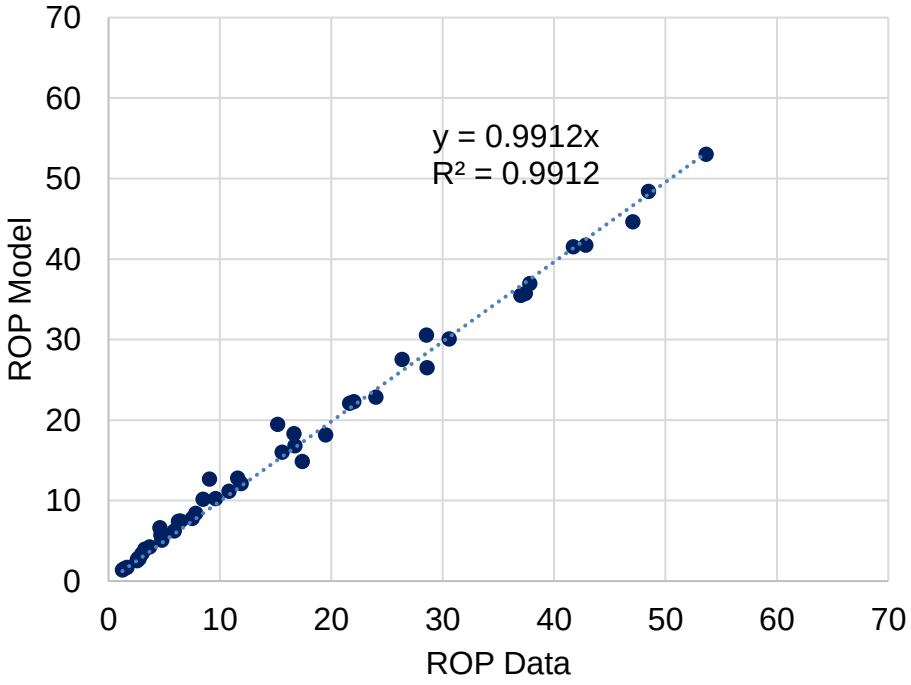

Figure 4.4: Comparison between approach one model estimated ROP and data (NOV 2019)

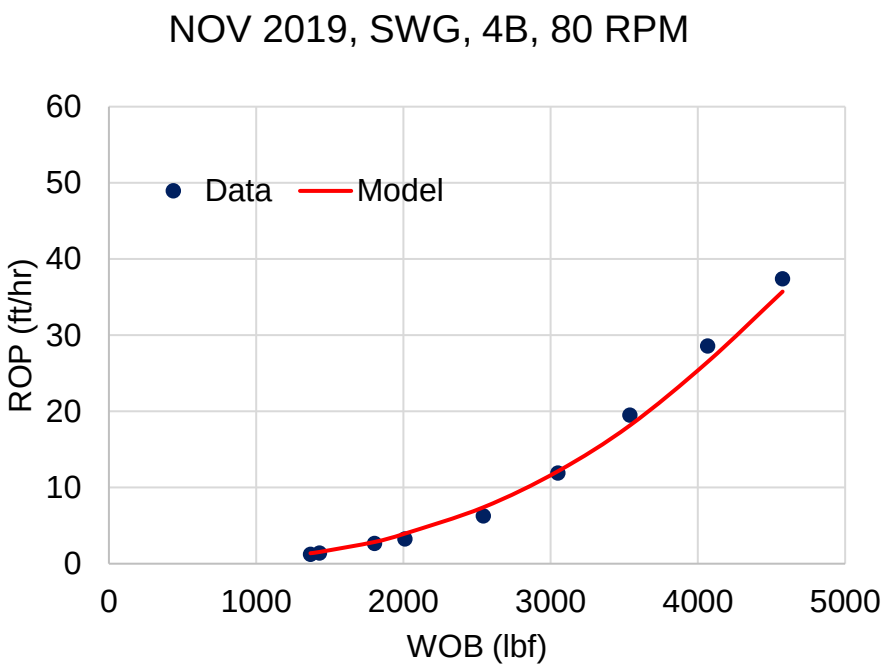

Figure 4.5: Comparison between approach one model estimated ROP and data for 4 bladed PDC bit at 80 RPM in SWG (NOV 2019)

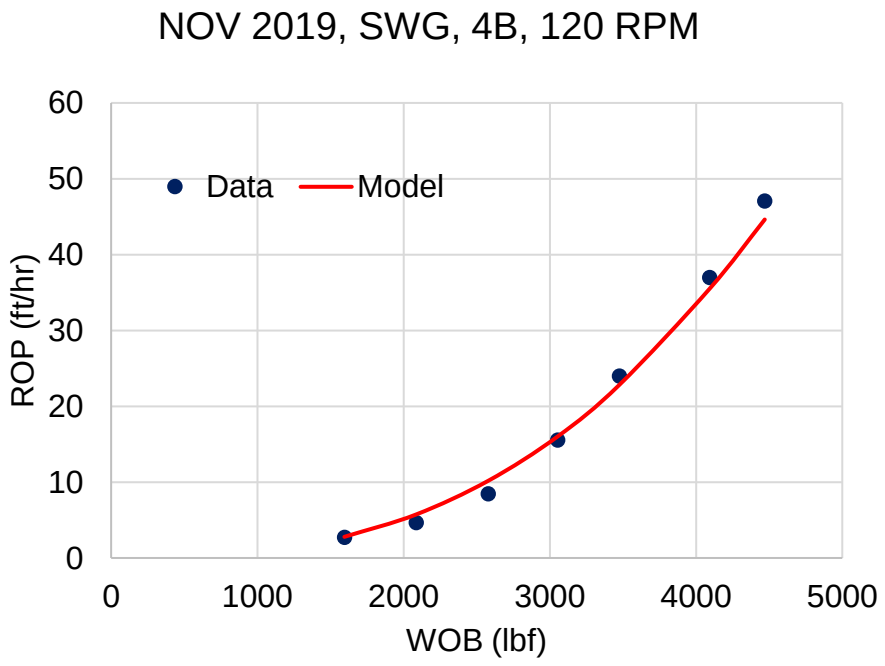

Figure 4.6: Comparison between approach one model estimated ROP and data for 4 bladed PDC bit at 120 RPM in SWG (NOV 2019)

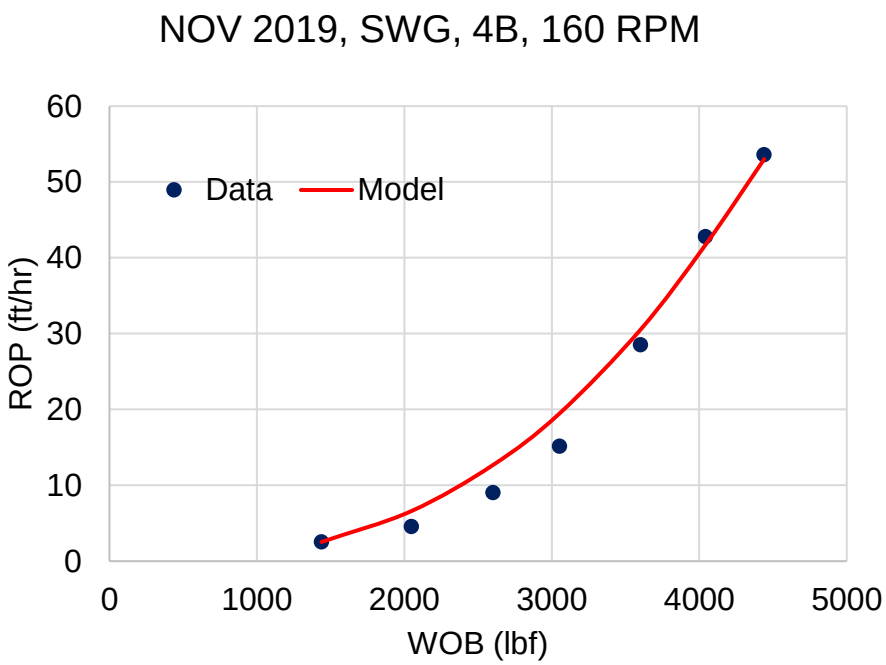

Figure 4.7: Comparison between approach one model estimated ROP and data for 4 bladed PDC bit at 160 RPM in SWG (NOV 2019)

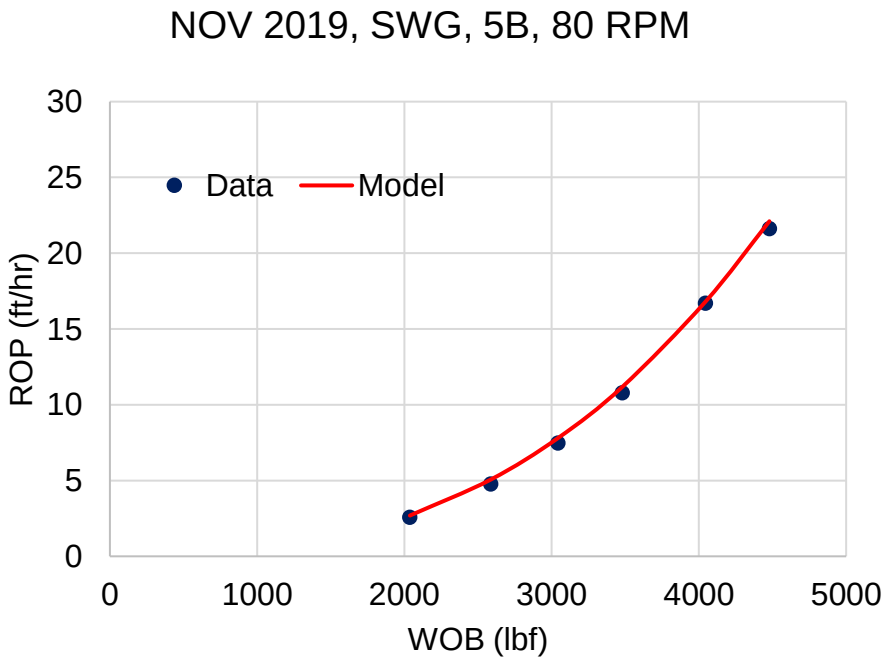

Figure 4.8: Comparison between approach one model estimated ROP and data for 5 bladed PDC bit at 80 RPM in SWG (NOV 2019)

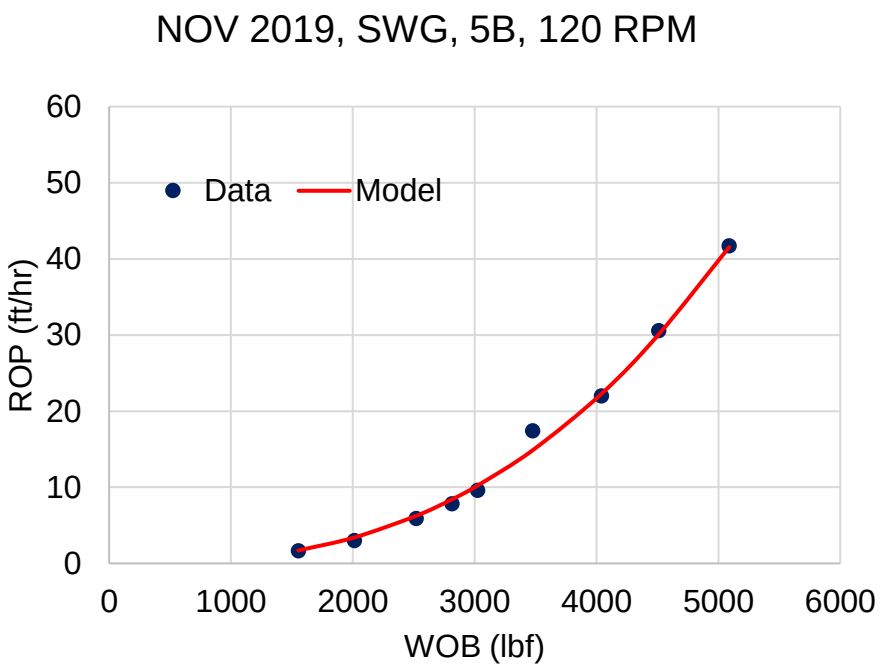

Figure 4.9: Comparison between approach one model estimated ROP and data for 5 bladed PDC bit at 120 RPM in SWG (NOV 2019)

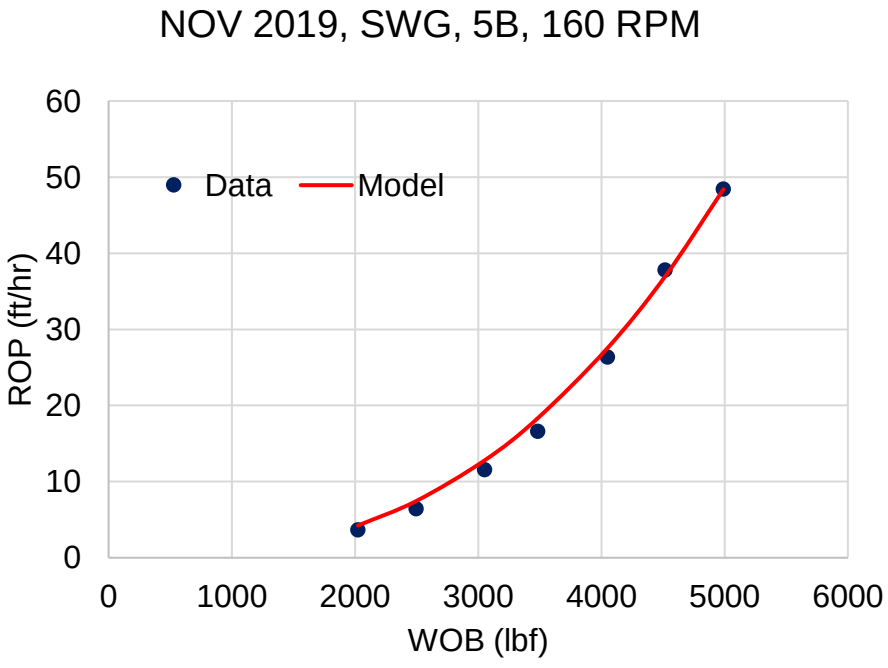

Figure 4.10: Comparison between approach one model estimated ROP and data for 5 bladed PDC bit at 160 RPM in SWG (NOV 2019)

Next, the approach two model was applied to the NOV 2019 data sets. The results of the approach two model are seen in Figures 4.11 through 4.17.

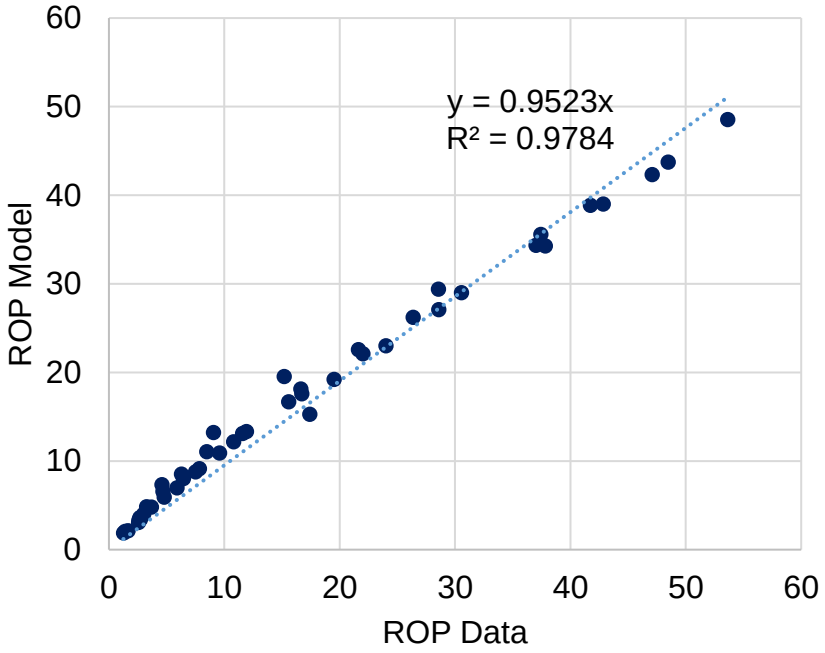

Figure 4.11: Comparison between approach two model estimated ROP and data (NOV 2019)

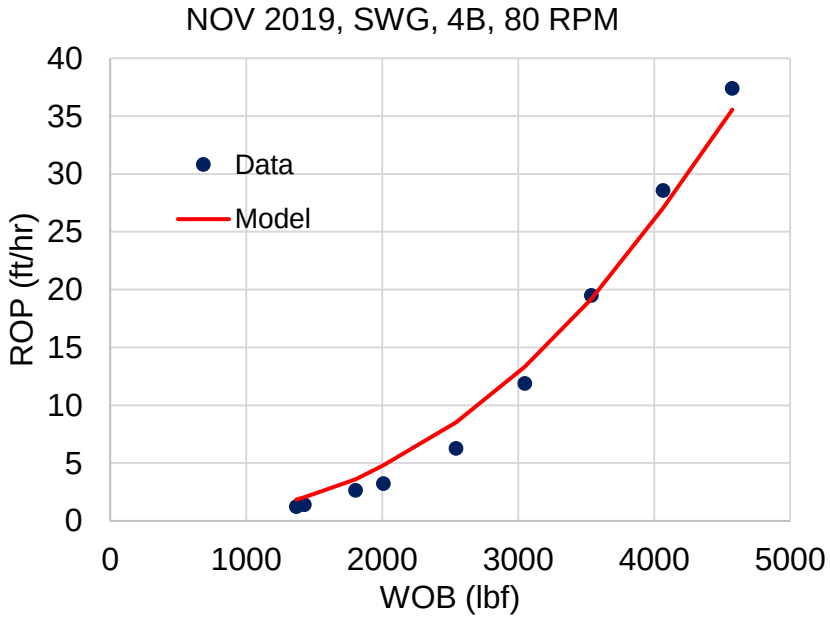

Figure 4.12: Comparison between approach two model estimated ROP and data for 4 bladed PDC bit at 80 RPM in SWG (NOV 2019)

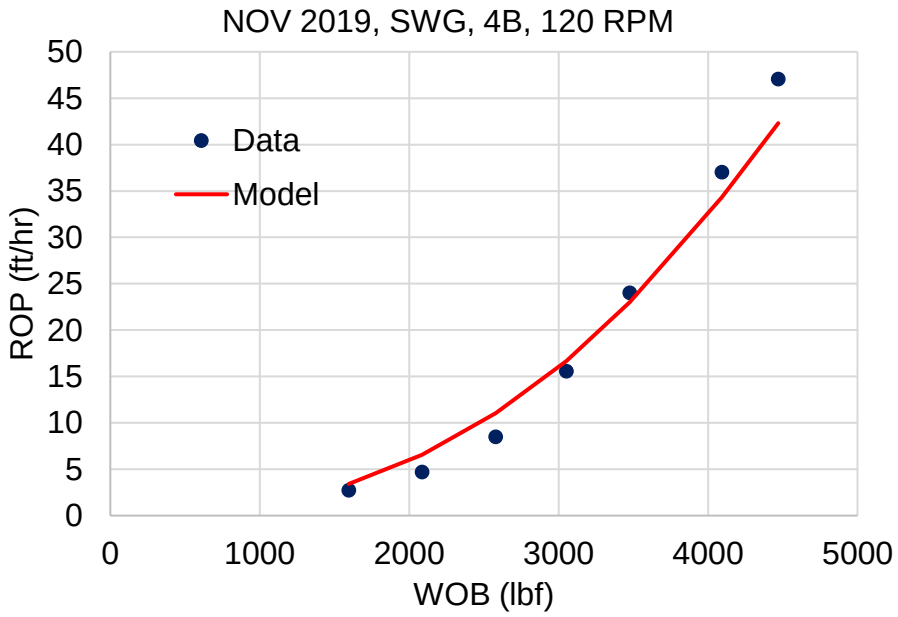

Figure 4.13: Comparison between approach two model estimated ROP and data for 4 bladed PDC bit at 120 RPM in SWG (NOV 2019)

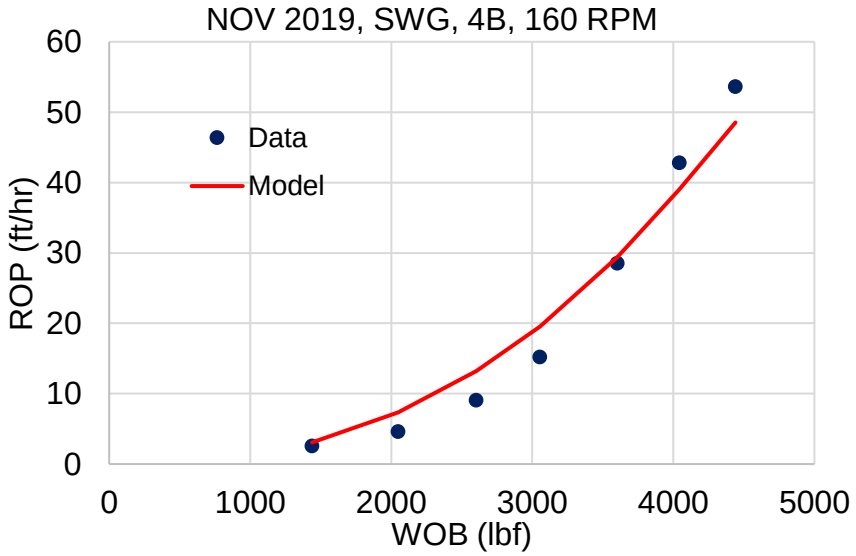

Figure 4.14: Comparison between approach two model estimated ROP and data for 4 bladed PDC bit at 160 RPM in SWG (NOV 2019)

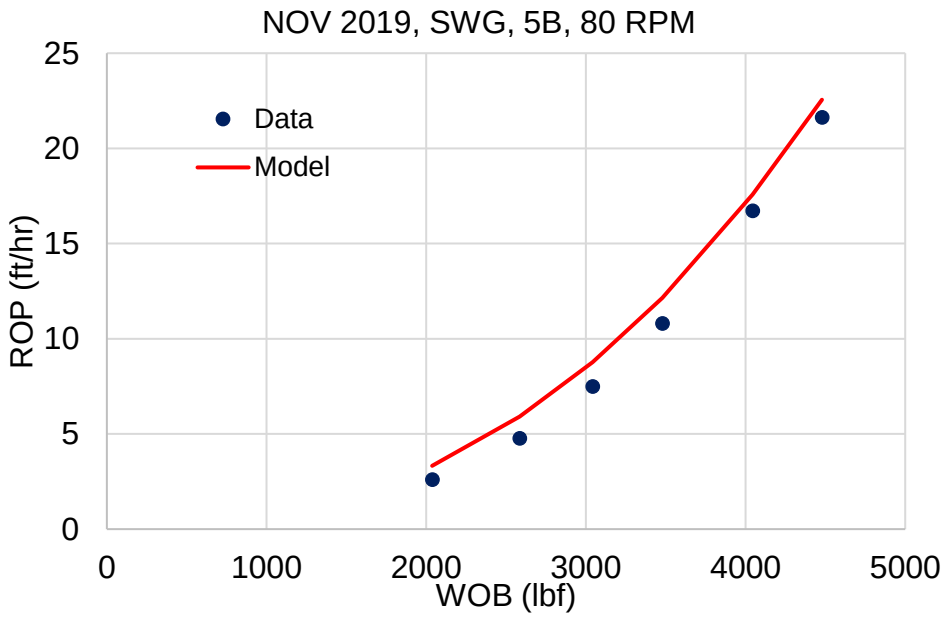

Figure 4.15: Comparison between approach two model estimated ROP and data for 5 bladed PDC bit at 80 RPM in SWG (NOV 2019)

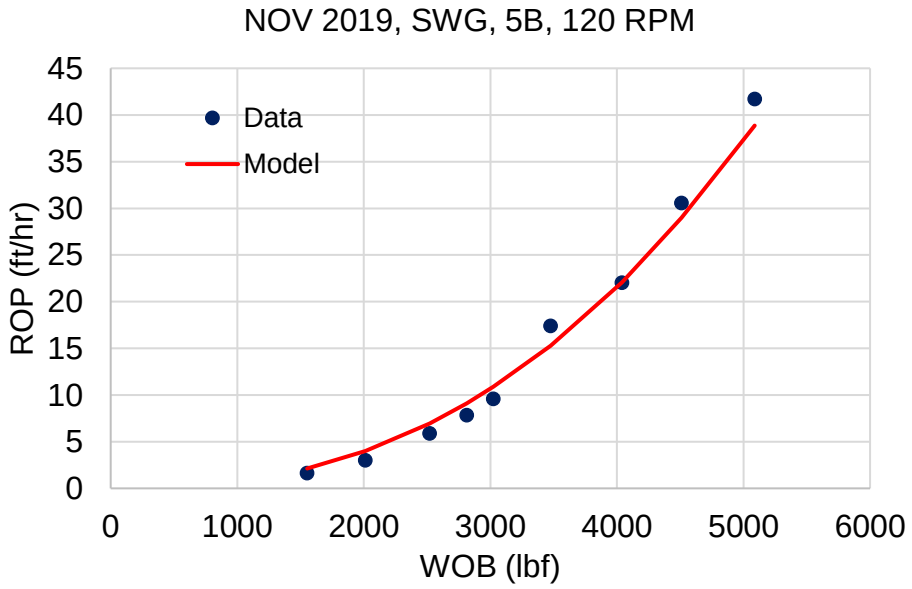

Figure 4.16: Comparison between approach two model estimated ROP and data for 5 bladed PDC bit at 120 RPM in SWG (NOV 2019)

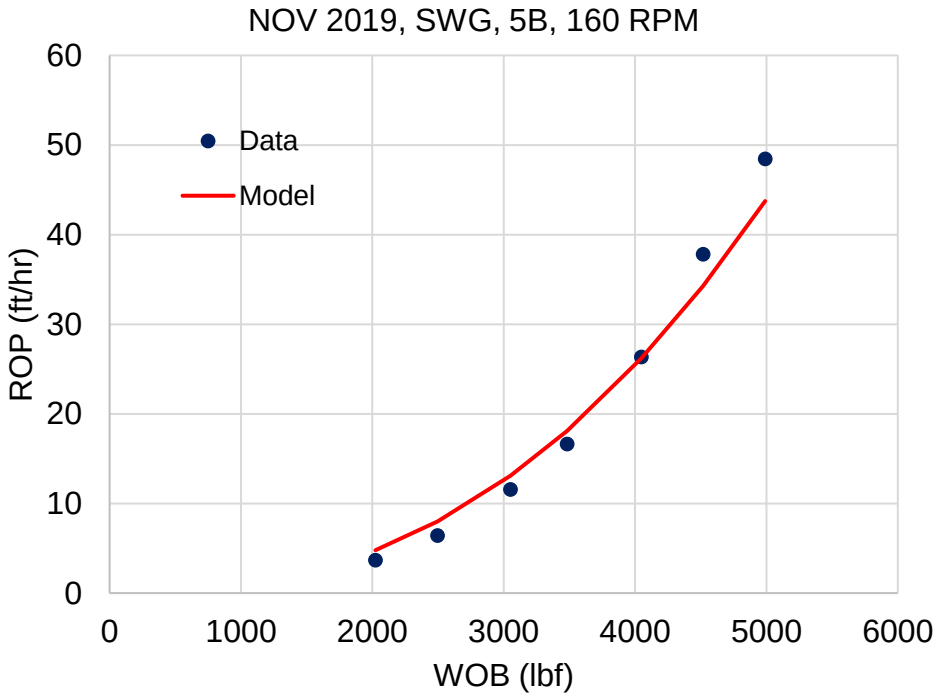

Figure 4.17: Comparison between approach two model estimated ROP and data for 5 bladed PDC bit at 160 RPM in SWG (NOV 2019)

As can be seen in the results, approach one appeared to be the more accurate model when applied to the new data set. This was a good verification that the model is accurate for phase I and phase II of the drilling phases just by calibrating the model with phase II data. Based on these findings, it can be concluded that all that is needed for calibrating the model for approach one is phase II drilling data.

4.3 Hydraulic Model Applied to the New PDC Drill Bit ROP Model

As stated in the calibration shown in section 3.3 that the model was interested in predicting phase II of the drilling process. This calibration method proved accurate for even phase I, but was unable to account for hydraulic inefficiencies. Applying the hydraulic function $(h(x))$ proved to enhance the models accuracy. To test this, a data set where phase III is in effect and bit

specifications needed for the hydraulic model need to be known. Hydraulic efficiencies were estimated for the Ulterra 4 blade as there was a bit specification sheet obtained that provided the parameters needed shown in the Equation 3.20. Since such similar testing conditions are met, it could be assumed that the hydraulic inefficiencies would occur at similar penetration rates for both studies. Moreover, the NOV 2019 data sets never achieved the needed WOB to initiated phase III so it could not be taken into account. The verification of approach one, including hydraulics, is shown below in Figures 4.18 through 4.20.

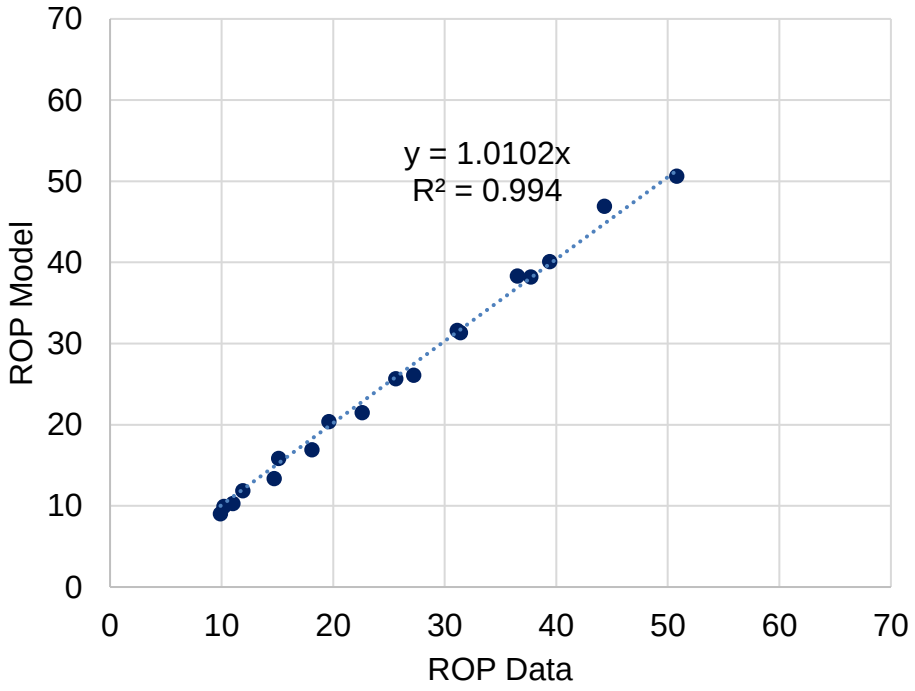

Figure 4.18: Comparison between approach one model estimated ROP including the hydraulic model and data (Raymond et al. 2015)

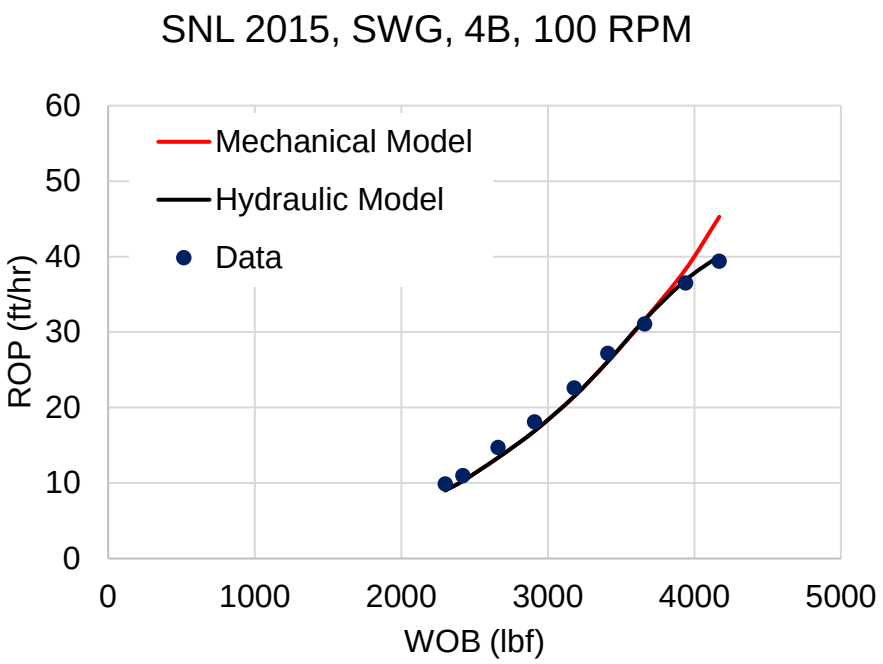

Figure 4.19: Comparison between approach one model estimated ROP including the hydraulic model and data for 4 bladed PDC bit at 100 RPM in SWG (Raymond et al. 2015)

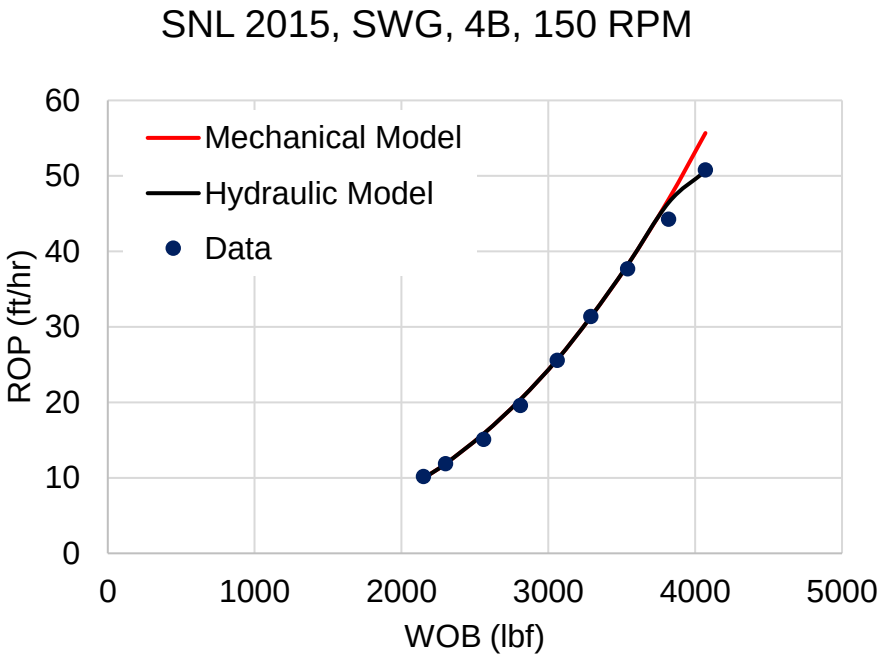

Figure 4.20: Comparison between approach one model estimated ROP including the hydraulic model and data for 4 bladed PDC bit at 150 RPM in SWG (Raymond et al. 2015)

4.4 Model Approach Decision

Based on the findings approach one is chosen as the optimal design for the model developed in this study. Though approach two was initially the more accurate model during the calibration process, applying the hydraulic model to approach one makes it the superior design for both data sets. The under estimation of Phase II data using approach two model rendered approach two unable to account for hydraulic efficiency.

When working with limited data sets, an understanding of physics and analyzing trends becomes vital for accurate model development. Approach two, which utilized the optimization algorithm, proved to be an optimal design within a limited data set whereas approach one accounted for future trends allowing hydraulics to be incorporated. Approach two would only increase in inaccurate results if the data sets were to continue on into higher recorded penetration rates.

CHAPTER VI

CONCLUSIONS

5.1 Summary

This study was taken up to develop a detailed PDC drill ROP model for hard rock and verifying using full hole data. The PDC drill bit ROP model shown was derived from single cutter analysis to incorporate physical parameters associated to PDC cutter performance. The approach taken to analyze PDC single cutter testing and provide verification of single cutter force modeling aided to begin a step by step process of full hole integration. From the ROP modeling analysis of this study, it can be concluded that the phase II data modeling is all that is needed to accurately predict PDC drill bit performance. Applying the calibrated approach one model to experimental data obtained and overseen by the OSU research team showed accurate results with less than 1% error during ideal cleaning conditions. Once hydraulics became a limiting factor, a hydraulics model was then applied which allowed for predications even after optimal cleaning efficiency was lost with less than 1% error as well. The findings and methods used to develop the new PDC drill bit model show potential for future use of creating real time drilling optimization systems using readily available operation parameters.

5.2 Future Work

To further the accuracy for the developed hard rock PDC drill bit ROP model variables that could be analyzed and included are cutter interaction, cutter material properties, different bit sizes, confining pressure, and drillability as mentioned in the literature. Additionally, the single cutter force modeling was only conducted for sharp cutters. An additional study to analyze the effects of the PDC cutter performance based on blunt cutters could indicate other parameters needed for increased accuracy. Including parameters such as these would complement the model to allow for more lithology variation and better predictions so that optimal drilling conditions could be met to continue reducing costs for drilling programs.

REFERENCES

1) Bellin, F. Dourfaye, A., King W., and Thigpen, M., (2010). “The Current State of PDC Bit Technology,” World Oil, 231(9), pp. 41–46.
2) Detournay, E. and Defourny, P. (1992) “A phenomenological model of the drilling action of drag bits.” International Journal of Rock Mechanics and Mining Sci. & Geomech. Abstr., 29(1):13-23
3) Detournay, Emmanuel, Thomas Richard, and Mike Shepherd (2008). "Drilling response of drag bits: theory and experiment". International Journal of Rock Mechanics and Mining Sciences45, no. 8 (2008): 1347-1360.
4) Dupriest, F. E., Witt, J. W., & Remmert, S. M. (2005). “Maximizing ROP With Real-Time Analysis of Digital Data and MSE.” International Petroleum Technology Conference. doi:10.2523/IPTC-10607-MS
5) Gerbaud, L., Menand, S., & Sellami, H. (2006). “PDC Bits: All Comes from the Cutter/Rock Interaction.” Society of Petroleum Engineers. doi:10.2118/98988-MS
6) Glowka, D.A. (1987). “Development of a method for predicting the performance and wear of PDC (polycrystalline diamond compact) drill bits.” United States. doi:10.2172/5591640.
7) Glowka, D. A. (1989). “Use of Single-Cutter Data in the Analysis of PDC Bit Designs: Part 1 - Development of a PDC Cutting Force Model. Society of Petroleum Engineers.” doi:10.2118/15619-PA
8) Hellvik, Svein, Runar Nygaard, Espen Hoel, Mats A. Andersen, and Mark Francis (2012). "PDC cutter and bit development for challenging conglomerate drilling in the Luno field-offshore Norway." In IADC/SPE Drilling Conference and Exhibition, 6-8 March, San Diego, California, USA
9) Hareland, G., & Rampersad, P. R. (1994). “Drag - Bit Model Including Wear. Society of Petroleum Engineers.” doi:10.2118/26957-MS
10) Hareland, G., Nygaard, R., Yan, W., & Wise, J. L. (2009). “Cutting Efficiency of a Single PDC Cutter on Hard Rock. Petroleum Society of Canada.” doi:10.2118/09-06-60
11) Huang, H. I., & Iversen, R. E. (1981). “The Positive Effects of Side Rake in Oilfield Bits Using Polycrystalline Diamond Compact Cutters. Society of Petroleum Engineers.” doi:10.2118/10152-MS

.

12) Holster, J. L., & Kipp, R. J. (1984). “Effect of Bit Hydraulic Horsepower on the Drilling Rate of a Polycrystalline Diamond Compact Bit. Society of Petroleum Engineers.” doi:10.2118/11949-PA
13) Kerkar, P. B., Hareland, G., Fonseca, E. R., & Hackbarth, C. J. (2014). “Estimation of Rock Compressive Strength Using Downhole Weight-on-Bit and Drilling Models.” International Petroleum Technology Conference. doi:10.2523/IPTC-17447-MS
14) Liou, J. (2012). “New bits look beyond design at overall wellbore.” Retrieved April 20, 2020, from https://www.drillingcontractor.org/new-bits-look-beyond-design-at-overall-wellbore-16693
15) Liu, J., Zheng, H., Kuang, Y., Xie, H., & Qin, C. (2019). “3D numerical simulation of rock cutting of an innovative non-planar face pdc cutter and experimental verification.” Applied Sciences, 9(20), 3-3. doi:10.3390/app9204372
16) Menand, S., and Gerbaud, L., 2005, “PDC Bit Technology Improvements Increase Efficiency, Bit Life,” Drilling Contractor Official Magazine, March/April, pp. 52–54.
17) Mensa-Wilmot, G., & Fear, M. J. (2001). “The Effects of Formation Hardness, Abrasiveness, Heterogeneity and Hole Size on PDC Bit Performance.” Society of Petroleum Engineers. doi:10.2118/67698-MS
18) Mensa-Wilmot, G., & Penrose, B. (2003). “Advanced Cutting Structure Improves PDC Bit Performance in Hard and Abrasive Drilling Environments. Society of Petroleum Engineers.” doi:10.2118/81167-MS
19) Motahhari, H. R., Hareland, G., & James, J. A. (2010). “Improved Drilling Efficiency Technique Using Integrated PDM and PDC Bit Parameters. Society of Petroleum Engineers.” doi:10.2118/141651-PA
20) Rahmani, R., Smith, J. R., & Taleghani, A. D. (2012). “Analytical Modeling of PDC Single Cutter-Rock Interaction Under Confining Pressure.” American Rock Mechanics Association.
21) Rahmani, Reza. (2013). “Analytical Modeling and Diagnosis of Penetration Rate Performance of PDC Bits”. Doctoral dissertation, Louisiana State University and Agricultural and Mechanical College.
22) Rajabov, V., Miska, S. Z., Mortimer, L., Yu, M., & Ozbayoglu, M. E. (2012). “The Effects of Back Rake and Side Rake Angles on Mechanical Specific Energy of Single PDC Cutters with Selected Rocks at Varying Depth of Cuts and Confining Pressures.” Society of Petroleum Engineers. doi:10.2118/151406-MS
23) Rampersad, P. R., Hareland, G., & Boonyapaluk, P. (1994). “Drilling Optimization Using Drilling Data and Available Technology.” Society of Petroleum Engineers. doi:10.2118/27034-MS
24) Raymond, D., Buerger, S., Cashion, A., Mesh, M., Radigan, W., and Su, J. (2015). “Active Suppression of Drilling System Vibrations for Deep Drilling (SAND2015-9432)”. Sandia National Laboratories (SNL-NM), Albuquerque, NM.
25) Sheikhnejad, Y., Rafati, A., & Sheikhnejad, F. (2014). “CFD Analysis of PDC Bit Heat Transfer by Drilling Mud Flow for Their Thermal Mortality.” The 5th National Conference on CFD Applications in Chemical & Petroleum Industries. Retrieved April 20, 2020 from https://www.researchgate.net/publication/312576118_CFD_Analysis_Of_PDC_Bit_Heat_Transfer_By_Drilling_Mud_Flow_For_Their_Thermal_Mortality.

26) Sinor, L. A., Powers, J. R., & Warren, T. M. (1998). “The Effect of PDC Cutter Density, Back Rake, Size, and Speed on Performance. Society of Petroleum Engineers.” doi:10.2118/39306-MS
27) Sinor, A., & Warren, T. M. (1989). “Drag Bit Wear Model. Society of Petroleum Engineers.” doi:10.2118/16699-PA
28) Warren, T. M., & Armagost, W. K. (1988). “Laboratory Drilling Performance of PDC Bits.” Society of Petroleum Engineers. doi:10.2118/15617-PA
29) Warren, T. M., & Sinor, A. (1989). “Drag-Bit Performance Modeling.” Society of Petroleum Engineers. doi:10.2118/15618-PA
30) Warren, T. M. (1987). “Penetration Rate Performance of Roller Cone Bits.” Society of Petroleum Engineers. doi:10.2118/13259-PA
31) Warren, T. M. (1981). “Drilling Model for Soft-Formation Bits. Society of Petroleum Engineers.” doi:10.2118/8438-PA
32) Wöhrl, T., & De Wall, H. (2002). “The onsite-geoscientist - handbook for drillsite geology.” Retrieved April 20, 2020, from https://www.researchgate.net/publication/262003381_The_onsite-geoscientist_-_Handbook_for_Drillsite_Geology.

APPENDIX A

Dc [inch]	DOC [inch]	UCS [psi]	Fn [lbf]	Fd [lbf]	Linear Velocity [inch/sec]	BR
0.5	0.017	21,500	31.7	26.3	2.2	20
0.5	0.015	21,500	25.3	16.8	2.2	20
0.5	0.016	21,500	30.4	17.0	2.2	20
0.5	0.018	21,500	29.2	18.8	2.2	20
0.5	0.013	21,500	23.9	16.9	2.2	20
0.5	0.020	21,500	38.0	28.9	2.2	20
0.5	0.039	21,500	131.0	118.0	2.2	20
0.5	0.039	21,500	136.0	120.0	2.2	20
0.5	0.039	21,500	137.0	121.0	2.2	20
0.5	0.037	21,500	136.0	118.0	2.2	20
0.5	0.061	21,500	229.0	217.0	2.2	20
0.5	0.062	21,500	256.0	227.0	2.2	20

Table A-1: Data from single cutter testing in Sierra White Granite report (Glowka 1987)

Dc [inch]	Nb	Nc	UCS [psi]	WOB [lbf]	Torque [ft.lb]	RPM	Db [inch]	BR	SR	ROP [ft/hr]
0.43	4	10	28000	2300	166	102	3.75	15	15	9.9
0.43	4	10	28000	2420	176	101	3.75	15	15	11
0.43	4	10	28000	2660	197	102	3.75	15	15	14.7
0.43	4	10	28000	2910	217	101	3.75	15	15	18.1
0.43	4	10	28000	3180	241	101	3.75	15	15	22.6
0.43	4	10	28000	3410	264	102	3.75	15	15	27.2
0.43	4	10	28000	3660	285	102	3.75	15	15	31.1
0.43	4	10	28000	3940	313	101	3.75	15	15	36.5
0.43	4	10	28000	4170	342	103	3.75	15	15	39.4
0.43	4	10	28000	2150	146	152	3.75	15	15	10.2
0.43	4	10	28000	2300	158	151	3.75	15	15	11.9
0.43	4	10	28000	2560	176	151	3.75	15	15	15.1
0.43	4	10	28000	2810	198	151	3.75	15	15	19.6
0.43	4	10	28000	3060	223	151	3.75	15	15	25.6
0.43	4	10	28000	3290	245	152	3.75	15	15	31.4
0.43	4	10	28000	3540	267	152	3.75	15	15	37.7
0.43	4	10	28000	3820	290	152	3.75	15	15	44.3
0.43	4	10	28000	4070	312	152	3.75	15	15	50.8
0.43	5	11	28000	2250	177	106	3.75	15	15	10.5
0.43	5	11	28000	2390	192	107	3.75	15	15	12.3
0.43	5	11	28000	2620	205	106	3.75	15	15	15.9
0.43	5	11	28000	2860	220	106	3.75	15	15	19.5
0.43	5	11	28000	3100	248	107	3.75	15	15	25.9
0.43	5	11	28000	3310	270	107	3.75	15	15	30.8
0.43	5	11	28000	3560	297	107	3.75	15	15	35.9
0.43	5	11	28000	3850	317	108	3.75	15	15	40.4
0.43	5	11	28000	4100	337	108	3.75	15	15	44.6
0.43	5	11	28000	2150	140	150	3.75	15	15	11.5
0.43	5	11	28000	2320	151	150	3.75	15	15	13.4
0.43	5	11	28000	2550	161	150	3.75	15	15	16.2
0.43	5	11	28000	2790	183	150	3.75	15	15	21.6
0.43	5	11	28000	3020	204	151	3.75	15	15	28.4
0.43	5	11	28000	3260	226	151	3.75	15	15	34.3
0.43	5	11	28000	3500	248	152	3.75	15	15	41.1
0.43	5	11	28000	3790	276	152	3.75	15	15	48.9
0.43	5	11	28000	4090	296	153	3.75	15	15	54.5

Table A-2: Data from 4 and 5 bladed bit data extracted from the SNL report (Raymond et al. 2015)

Dc [inch]	Nb	Nc	UCS [psi]	WOB [lbf]	Torque [ft.lb]	RPM	Db [inch]	BR	SR	ROP [ft/hr]
0.51	4	11	28000	1369	89	80	3.75	25	1	1.2
0.51	4	11	28000	1430	89	79	3.75	25	1	1.4
0.51	4	11	28000	1805	123	78	3.75	25	1	2.7
0.51	4	11	28000	2010	140	82	3.75	25	1	3.2
0.51	4	11	28000	2544	190	81	3.75	25	1	6.3
0.51	4	11	28000	3049	256	82	3.75	25	1	11.9
0.51	4	11	28000	3539	320	82	3.75	25	1	19.5
0.51	4	11	28000	4067	372	82	3.75	25	1	28.6
0.51	4	11	28000	4575	427	80	3.75	25	1	37.4
0.51	4	11	28000	1595	95	122	3.75	25	1	2.7
0.51	4	11	28000	2085	131	121	3.75	25	1	4.7
0.51	4	11	28000	2580	170	121	3.75	25	1	8.5
0.51	4	11	28000	3053	219	121	3.75	25	1	15.6
0.51	4	11	28000	3476	273	122	3.75	25	1	24.0
0.51	4	11	28000	4093	337	122	3.75	25	1	37.0
0.51	4	11	28000	4470	380	120	3.75	25	1	47.1
0.51	4	11	28000	1438	83	159	3.75	25	1	2.6
0.51	4	11	28000	2048	110	159	3.75	25	1	4.6
0.51	4	11	28000	2601	152	161	3.75	25	1	9.1
0.51	4	11	28000	3052	191	160	3.75	25	1	15.2
0.51	4	11	28000	3603	257	161	3.75	25	1	28.5
0.51	4	11	28000	4043	305	161	3.75	25	1	42.8
0.51	4	11	28000	4440	350	158	3.75	25	1	53.6
0.43	5	16	28000	2037	91	81	3.75	27	1	2.6
0.43	5	16	28000	2586	122	80	3.75	27	1	4.8
0.43	5	16	28000	3043	151	79	3.75	27	1	7.5
0.43	5	16	28000	3480	179	79	3.75	27	1	10.8
0.43	5	16	28000	4045	224	79	3.75	27	1	16.7
0.43	5	16	28000	4479	259	79	3.75	27	1	21.6
0.43	5	16	28000	1552	69	120	3.75	27	1	1.6
0.43	5	16	28000	2012	87	119	3.75	27	1	3.0
0.43	5	16	28000	2521	115	119	3.75	27	1	5.9
0.43	5	16	28000	2814	133	120	3.75	27	1	7.8
0.43	5	16	28000	3024	145	120	3.75	27	1	9.6
0.43	5	16	28000	3475	175	119	3.75	27	1	17.4
0.43	5	16	28000	4041	215	119	3.75	27	1	22.0
0.43	5	16	28000	4511	253	120	3.75	27	1	30.6
0.43	5	16	28000	5088	300	119	3.75	27	1	41.7
0.43	5	16	28000	2024	91	160	3.75	27	1	3.7
0.43	5	16	28000	2496	115	159	3.75	27	1	6.4
0.43	5	16	28000	3053	147	159	3.75	27	1	11.6
0.43	5	16	28000	3482	173	160	3.75	27	1	16.6
0.43	5	16	28000	4049	212	160	3.75	27	1	26.4
0.43	5	16	28000	4518	249	160	3.75	27	1	37.8
0.43	5	16	28000	4990	284	160	3.75	27	1	48.5

Table A-3: Data from 4 and 5 bladed bit data extracted from the SNL report (NOV 2019)

VITA

Seth Colton Sleeper

Candidate for the Degree of

Master of Science

Thesis: PDC DRILL BIT MODELING IN HARD ROCK

Major Field: Petroleum Engineering

Biographical:

Education:

Rose State College — Fall 2014 – Spring 2015
AA: Mechanical Engineering

Oklahoma State University — Fall 2015 – Spring 2018
BS: Mechanical Engineering

Oklahoma State University — Fall 2018 – Spring 2020
MS: Petroleum Engineering

Experience:

Ulterra Drilling Technologies — Summer 2018
Failure analysis engineering looking at matrix body bit design and nozzle optimization. Created road maps for drilling parameters for field applications.

Ascent Resources — Summer 2019
Worked in Utica basin in the completions team to evaluate innovative frac and wireline technologies.

Professional Memberships:
Society of Petroleum Engineering
American Association of Drilling Engineers